Chapter 4 Ore Reserve Calculation

4-1 Objective

The objective of the ore reserve calculation is to assess the mineral potential of the survey area.

4-2 Method

The calculation was carried out by ZCCM using LYNX computer of Canadian LYNX GEOSYSTEM INC.

Kriging method, Inverse Distance Squared method and manual calculation on orebody sections were studied for the ore reserve calculation. In the Kriging, borehole data points may not be enough for constructing a reliable semi-variogram, while the manual calculation overestimated the tonnage and the grade in the part of low density of borehole. Consequently Inverse Distance Squared method was adopted to the ore reserve calculation of the area.

In the Inverse Distance Squared method the grade of a block is calculated that:

$$X=\sum_{i=1}^{N}(xi/di^2)\ /\ \sum_{i=1}^{N}(1/di^2)$$

X : block grade
xi: grade composite value of neighbouring sample point (intersection grade of drill hole etc.)
di: distance between centre of block and sample point
i : neighbouring sample point
N : number of samples used for the estimation

Inverse Distance Squared method was used under the following conditions.

3D GRID MODEL DIMENSIONS: 150 x 150 x 1300 (m)
SEARCH ELLIPSOID DIMENSIONS: 800 x 800 x 800 (m)
CUT-OFF GRADE: 1% T-Cu
ORE DENSITY: 2.67

Assay results of gold and silver for the intersections of drill holes are listed in the appendices. These results are generally low (in the order of ppb). However, there are several relatively high grade ores in some part of the Southern Area Shoot, Northern Area Shoot and in the western part of the survey area. The matter how to treat these gold and silver assays in the calculation of ore reserves are now being discussed by ZCCM.

4-3 Results

68 boreholes were found to have intersections of 1% Cu mineralization.

The orebody being mostly gentle slope lying, each 3D Grid cell created one orebody intersection as seen in the plan.

Figures and tables of various kinds on the results of the calculation are shown in appendices.

ZCCM has made a policy not to use the word ore unless an economic evaluation has been made, and concluded that the tonnage and grade of the results be expressed under two headings:

(A) Potentially Economic Mineralization: This will be summation of blocks which have a minimum true thickness of 3m and a minimum block grade of 2% t-Cu. The blocks should also be connected with each other making a minable body. This criterion was used to quantify the Northern Area Shoot and the Southern Area Shoot.

(B) Subeconomic mineralization: The grade and tonnage of the remaining blocks of the 1% Cut-Off mineralization.

The areas around NN-75, MJZC-9(NN-84) and RCB-2 were purposely left out from the Potentially Economic Mineralization as those are separated from the Northern Area Shoot and require further drilling to firm up the block grades and tonnages. However those areas are regarded as of considerable promise for location of economic mineralization.

The tonnages and grades of the survey area are as follows.

POTENTIALLY ECONOMIC MINERALIZATION;
NORTHERN AREA SHOOT: 54,793,000 tons, 2.70% T-Cu, 0.13% T-Co
SOUTHERN AREA SHOOT: 14,934,000 tons, 2.19% T-Cu, 0.13% T-Co

SUBECONOMIC MINERALIZATION (includes isolated patches of 2% Cu and 3m true thickness blocks):

107,909,000 tons, 1.83% T-Cu, 0.03% T-Co

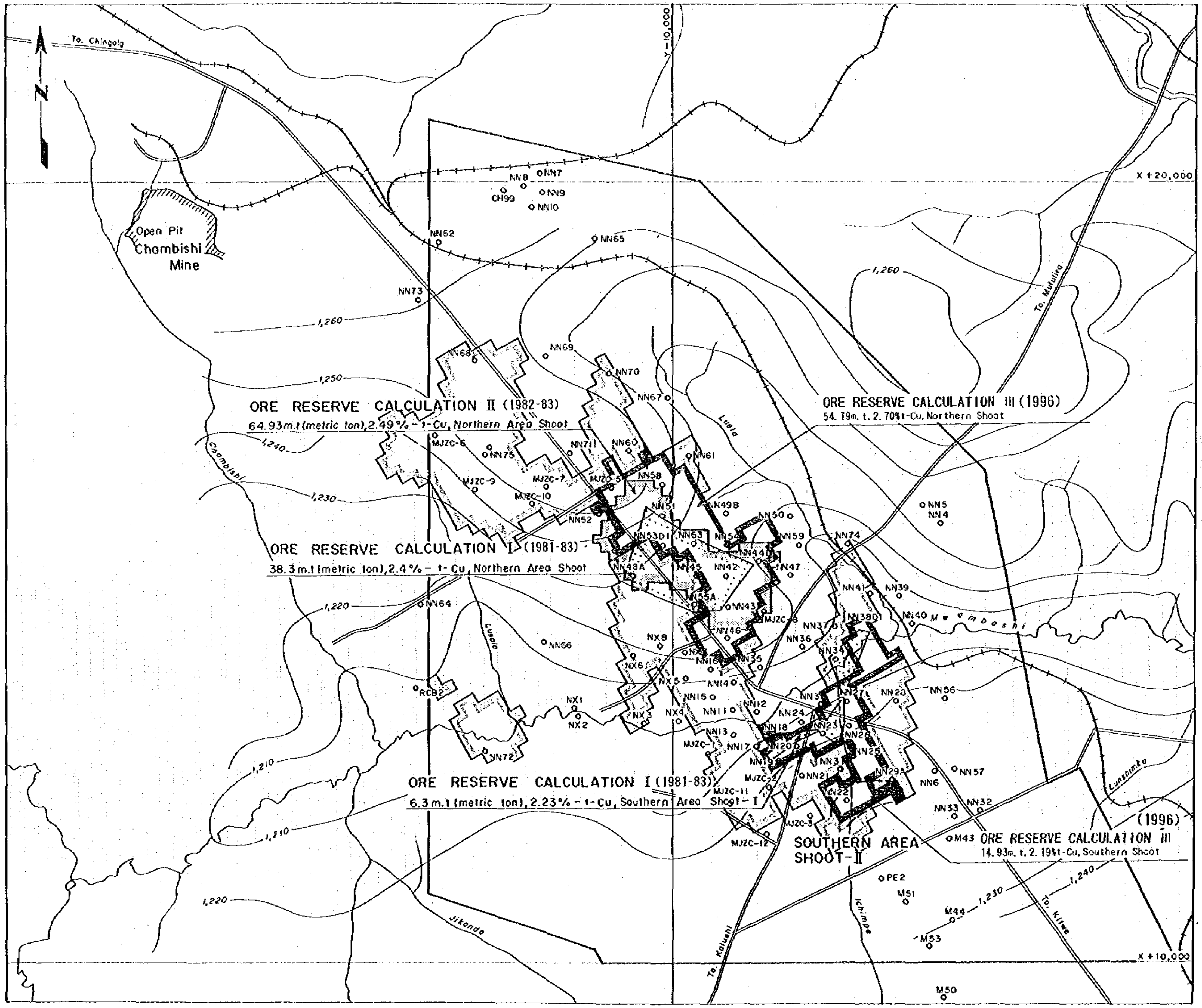

LEGEND

o Drilling Holes

Topographic Elevation Contour in Metre (1,260; 1,250)

Survey Area

ORE RESERVE CALCULATION III (1996)

Subeconomic Blocks, 10.91m.t, 1.83%t-Cu

Northern Area Shoot

	True Thickness (m)	Total Cu%	Total Co%
NN58	22.92	2.21	0.09
51	14.21	2.68	0.06
48-B	4.67	2.07	0.02
53-D1	4.92	2.15	0.05
63	18.41	2.11	0.21
45	10.39	2.32	0.06
42	16.27	2.29	0.10
44-D1	15.90	2.86	0.18
55-A	3.02	2.04	0.04
43	12.02	2.93	0.09

Southern Area Shoot-I

	True Thickness (m)	Total Cu%	Total Co%
NN11	5.49	1.88	0.04
NN18	4.48	2.81	0.07
20	5.06	1.92	0.13
23	4.75	2.62	0.27
26	4.63	1.87	0.12
27	5.12	2.31	0.28
38-D1	3.90	2.98	0.01
40	9.78	2.17	0.04

Southern Area Shoot-II

	True Thickness (m)	Total Cu%	Total Co%
NN22	5.61	2.37	0.13
29	9.08	1.75	0.17

Nothwestern Area

	True Thikness (m)	Total Cu%	Total Co%
NN75	10.72	2.11	0.09
MJZC-9	5.79	3.12	0.08

Fig. 2-4-1 Ore Reserve Calculation

Table 2-5-1 Results of Chemical Analysis of Ore Samples (1)

MJZC−1

Sample No.	Depth (m)	T-Cu (%)	T-Co (%)	AS-Cu (%)
LC14323	499.53 ~ 500.03	<0.01	<0.01	<0.01
LC14324	500.03 ~ 500.53	<0.01	<0.01	<0.01
LC14325	500.53 ~ 501.03	<0.01	<0.01	<0.01
LC14326	501.03 ~ 501.53	<0.01	<0.01	<0.01
LC14327	501.53 ~ 502.03	<0.01	<0.01	<0.01
LC14328	502.03 ~ 502.53	<0.01	<0.01	<0.01
LC14329	502.53 ~ 502.90	<0.01	<0.01	<0.01
LC14330	502.90 ~ 503.40	<0.01	<0.01	<0.01
LC14331	503.40 ~ 503.90	<0.01	<0.01	<0.01
LC14332	503.90 ~ 504.40	<0.01	<0.01	<0.01
LC14333	504.40 ~ 504.90	<0.01	<0.01	<0.01
LC14334	504.90 ~ 505.53	<0.01	<0.01	<0.01
LC14335	505.53 ~ 506.03	<0.01	0.02	<0.01
LC14336	506.03 ~ 506.53	<0.01	0.02	<0.01
LC14337	506.53 ~ 507.03	<0.01	0.03	<0.01
LC14338	507.03 ~ 507.53	<0.01	0.06	<0.01
LC14339	507.53 ~ 508.03	0.02	0.02	<0.01
LC14340	508.03 ~ 508.20	0.01	0.03	<0.01
LC14341	508.20 ~ 508.70	<0.01	0.05	<0.01
LC14342	508.70 ~ 509.20	<0.01	0.03	<0.01
LC14343	509.20 ~ 509.70	<0.01	0.03	<0.01
LC14344	509.70 ~ 510.20	0.01	0.03	<0.01
LC14345	510.20 ~ 510.70	<0.01	0.03	<0.01
LC14346	510.70 ~ 511.20	0.02	0.04	<0.01
LC14347	511.20 ~ 511.53	0.02	0.04	<0.01
LC14348	511.53 ~ 512.03	0.07	0.05	<0.01
LC14349	512.03 ~ 512.53	0.05	0.02	<0.01
LC14350	512.53 ~ 513.03	0.32	0.02	<0.01
LC14351	513.03 ~ 513.53	0.32	0.01	<0.01
LC14352	513.53 ~ 514.03	0.11	<0.01	<0.01
LC14353	514.03 ~ 514.53	0.11	<0.01	<0.01
LC14354	514.53 ~ 515.03	0.13	0.01	<0.01
LC14355	515.03 ~ 515.26	0.07	<0.01	<0.01
LC14356	515.26 ~ 515.76	0.25	0.02	<0.01
LC14357	515.76 ~ 516.26	0.10	0.01	<0.01
LC14358	516.26 ~ 516.76	0.19	0.01	<0.01
LC14359	516.76 ~ 516.99	0.21	0.05	<0.01
LC14360	516.99 ~ 517.53	0.92	0.02	<0.01
LC14361	517.53 ~ 518.03	0.19	0.02	<0.01
LC14362	518.03 ~ 518.53	0.12	0.05	<0.01
LC14363	518.53 ~ 519.03	0.31	0.06	<0.01
LC14364	519.03 ~ 519.53	0.23	0.11	<0.01
LC14365	519.53 ~ 520.03	0.07	0.07	<0.01
LC14366	520.03 ~ 520.53	0.05	0.04	<0.01
LC14367	520.53 ~ 520.93	0.02	0.02	<0.01
LC14368	520.93 ~ 521.18	0.02	0.04	<0.01
LC14369	521.18 ~ 521.68	0.38	0.01	<0.01
LC14370	521.68 ~ 522.18	0.48	0.01	<0.01
LC14371	522.18 ~ 522.68	0.59	0.01	<0.01
LC14372	522.68 ~ 523.18	0.61	<0.01	<0.01
LC14373	523.18 ~ 523.53	0.41	<0.01	<0.01
LC14374	523.53 ~ 524.03	0.88	<0.01	<0.01
LC14375	524.03 ~ 524.23	0.72	<0.01	<0.01
LC14376	524.23 ~ 524.53	0.59	0.01	<0.01
LC14377	524.53 ~ 525.03	0.55	0.02	<0.01
LC14378	525.03 ~ 525.53	0.40	<0.01	<0.01
LC14379	525.53 ~ 526.03	0.25	<0.01	<0.01
LC14380	526.03 ~ 526.53	0.24	<0.01	<0.01
LC14381	526.53 ~ 527.03	0.24	<0.01	<0.01
LC14382	527.03 ~ 527.53	0.31	0.01	<0.01
LC14383	527.53 ~ 528.03	0.23	0.01	<0.01
LC14384	528.03 ~ 528.53	0.06	<0.01	<0.01
LC14385	528.53 ~ 529.03	0.09	<0.01	<0.01
LC14386	529.03 ~ 529.53	0.08	<0.01	<0.01
LC14387	529.53 ~ 530.03	0.09	<0.01	<0.01
LC14388	530.03 ~ 530.53	0.07	<0.01	<0.01
LC14389	530.53 ~ 530.83	0.02	<0.01	<0.01

Width (m)	Depth (m)	T-Cu %	AS-Cu %	T-Co (%)
2.85	552.18 ~ 525.03	0.62	<0.01	<0.01

MJZC−2

Sample No.	Depth (m)	T-Cu (%)	AS-Cu (%)	T-Co (%)	As-Co (%)	Ni ppm	Zn ppm
KC15160	638.29 ~ 638.62	<0.01	<0.01	0.01	<0.01	50	21
KC15161	638.62 ~ 639.12	<0.01	<0.01	0.02	<0.01	42	17
KC15162	639.12 ~ 639.62	<0.01	<0.01	0.09	<0.01	44	8
KC15163	639.62 ~ 640.12	<0.01	<0.01	0.04	<0.01	48	18
KC15164	640.12 ~ 640.62	<0.01	<0.01	0.03	<0.01	47	9
KC15165	640.62 ~ 641.12	<0.01	<0.01	0.02	<0.01	59	12
KC15166	641.12 ~ 641.62	<0.01	<0.01	0.03	<0.01	52	11
KC15167	641.62 ~ 642.12	0.01	<0.01	0.03	<0.01	44	9
KC15168	642.12 ~ 642.62	<0.01	<0.01	0.02	<0.01	45	9
KC15169	642.62 ~ 643.12	<0.01	<0.01	0.03	<0.01	48	10
KC15170	643.12 ~ 643.62	<0.01	<0.01	0.02	<0.01	42	10
KC15171	643.62 ~ 644.12	<0.01	<0.01	0.02	<0.01	47	13
KC15172	644.12 ~ 644.62	<0.01	<0.01	0.04	<0.01	45	12
KC15173	644.62 ~ 645.12	<0.01	<0.01	0.03	<0.01	45	12
KC15174	645.12 ~ 645.62	<0.01	<0.01	0.04	<0.01	45	13
KC15175	645.62 ~ 646.12	0.05	<0.01	0.06	<0.01	39	11
KC15176	646.12 ~ 646.62	0.02	<0.01	0.05	<0.01	48	8
KC15177	646.62 ~ 647.12	0.05	<0.01	0.06	<0.01	41	9
KC15178	647.12 ~ 647.62	0.07	<0.01	0.05	<0.01	39	10
KC15179	647.62 ~ 648.12	0.29	<0.01	0.02	<0.01	42	10
KC15180	648.12 ~ 648.62	0.47	<0.01	0.05	<0.01	41	18
KC15181	648.62 ~ 649.12	0.14	<0.01	0.01	<0.01	32	18
KC15182	649.12 ~ 649.62	0.46	<0.01	0.02	<0.01	43	33
KC15183	649.62 ~ 650.07	0.49	<0.01	0.03	<0.01	47	27
KC15184	650.07 ~ 650.57	0.28	<0.01	0.02	<0.01	38	22
KC15185	650.57 ~ 651.07	0.36	<0.01	0.03	<0.01	38	23
KC15186	651.07 ~ 651.57	0.64	0.01	0.02	<0.01	37	31
KC15187	651.57 ~ 652.07	0.66	<0.01	0.03	<0.01	38	97
KC15188	652.07 ~ 652.66	0.58	<0.01	0.05	<0.01	52	115
KC15189	652.66 ~ 652.83	1.62	<0.01	0.07	<0.01	45	139
KC15190	652.83 ~ 653.33	0.83	<0.01	0.05	<0.01	45	139
KC15191	653.33 ~ 653.83	0.49	<0.01	0.02	<0.01	28	115
KC15192	653.83 ~ 654.33	6.86	0.02	0.12	<0.01	70	335
KC15193	654.33 ~ 654.83	0.73	<0.01	0.04	<0.01	37	45
KC15194	654.83 ~ 655.33	1.02	<0.01	0.05	<0.01	33	56
KC15195	655.33 ~ 655.83	3.13	<0.01	0.21	<0.01	40	149
KC15196	655.83 ~ 655.97	1.00	<0.01	0.09	<0.01	37	51
KC15197	655.97 ~ 656.47	0.83	<0.01	0.10	<0.01	35	55
KC15198	656.47 ~ 656.97	1.03	<0.01	0.21	<0.01	60	51
KC15199	656.97 ~ 657.25	0.77	<0.01	0.09	<0.01	33	39
KC15200	657.25 ~ 657.75	0.37	<0.01	0.03	<0.01	32	30
KC19784	657.75 ~ 658.25	0.07	<0.01	0.04	<0.01	22	24
KC19785	658.25 ~ 658.43	0.46	<0.01	0.03	<0.01	29	28
KC19786	658.43 ~ 658.51	0.21	<0.01	0.12	<0.01	30	21
KC19787	658.51 ~ 659.01	<0.01	<0.01	<0.01	<0.01	27	12
KC19788	659.01 ~ 659.51	<0.01	<0.01	<0.01	<0.01	28	13
KC19789	659.51 ~ 660.01	<0.01	<0.01	<0.01	<0.01	23	13
KC19790	660.01 ~ 660.51	0.01	<0.01	<0.01	<0.01	23	11
KC19791	660.51 ~ 661.01	<0.01	<0.01	<0.01	<0.01	26	22
KC19792	661.01 ~ 661.51	<0.01	<0.01	<0.01	<0.01	30	20
KC19793	661.51 ~ 661.97	<0.01	<0.01	<0.01	<0.01	18	18

Width (m)	Depth (m)	T-Cu (%)	As-Cu (%)	T-Co (%)
3.14	653.83 ~ 656.97	2.21	<0.01	0.12

Table 2-5-1 Results of Chemical Analysis of Ore Samples (2)

MJZC-3

Sample No.	Depth (m)	T-Cu (%)	AS-Cu (%)	T-Co (%)	AS-Co (%)
KC19701	632.47 ~ 632.66	<0.01	<0.01	<0.01	<0.01
KC19702	632.66 ~ 633.13	<0.01	<0.01	<0.01	<0.01
KC19703	633.13 ~ 633.63	<0.01	<0.01	<0.01	<0.01
KC19704	633.63 ~ 634.13	<0.01	<0.01	<0.01	<0.01
KC19705	634.13 ~ 634.63	<0.01	<0.01	<0.01	<0.01
KC19706	634.63 ~ 634.84	<0.01	<0.01	<0.01	<0.01
KC19707	634.84 ~ 635.03	<0.01	<0.01	<0.01	<0.01
KC19708	635.03 ~ 635.32	<0.01	<0.01	0.02	<0.01
KC19709	635.32 ~ 635.61	<0.01	<0.01	0.02	<0.01
KC19710	635.61 ~ 635.94	<0.01	<0.01	0.03	<0.01
KC19711	635.94 ~ 636.31	0.80	<0.01	0.02	<0.01
KC19712	636.31 ~ 636.81	1.16	<0.01	<0.01	<0.01
KC19713	636.81 ~ 637.31	0.34	<0.01	0.02	<0.01
KC19714	637.31 ~ 637.81	0.05	<0.01	0.01	<0.01
KC19715	637.81 ~ 638.31	0.06	<0.01	0.01	<0.01
KC19716	638.31 ~ 638.81	0.02	<0.01	0.01	<0.01
KC19717	638.81 ~ 639.31	<0.01	<0.01	<0.01	<0.01
KC19718	639.31 ~ 639.81	0.01	<0.01	<0.01	<0.01
KC19719	639.81 ~ 640.31	0.02	<0.01	0.01	<0.01
KC19720	640.31 ~ 640.66	<0.01	<0.01	0.01	<0.01
KC19721	640.66 ~ 640.84	0.02	<0.01	0.02	<0.01
KC19722	640.84 ~ 641.34	0.02	<0.01	0.03	<0.01
KC19723	641.34 ~ 641.84	0.03	<0.01	0.03	<0.01
KC19724	641.84 ~ 642.26	0.06	<0.01	0.03	<0.01
KC19725	642.26 ~ 642.79	0.30	<0.01	0.03	<0.01
KC19726	642.79 ~ 643.29	0.01	<0.01	0.03	<0.01
KC19727	643.29 ~ 643.8	0.01	<0.01	0.03	<0.01
KC19728	643.80 ~ 644.31	0.11	<0.01	0.08	<0.01
KC19729	644.31 ~ 644.74	0.80	0.01	0.09	<0.01
KC19730	644.74 ~ 645.24	1.09	0.01	0.06	<0.01
KC19731	645.24 ~ 645.72	0.22	<0.01	0.05	<0.01
KC19732	645.72 ~ 646.23	0.42	<0.01	0.05	<0.01
KC19733	646.23 ~ 646.73	0.78	<0.01	0.04	<0.01
KC19734	646.73 ~ 647.23	0.55	<0.01	0.07	<0.01
KC19735	647.23 ~ 647.73	0.45	<0.01	0.06	<0.01
KC19736	647.73 ~ 648.23	2.51	0.04	0.27	<0.01
KC19737	648.23 ~ 648.73	1.38	0.01	0.12	<0.01
KC19738	648.73 ~ 649.23	0.92	<0.01	0.20	<0.01
KC19739	649.23 ~ 649.73	1.32	0.01	0.11	<0.01
KC19740	649.73 ~ 649.84	1.62	0.02	0.31	<0.01
KC19741	649.84 ~ 650.13	0.02	0.01	0.23	<0.01
KC19742	650.13 ~ 650.42	<0.01	<0.01	0.01	<0.01
KC19743	650.42 ~ 650.71	<0.01	<0.01	0.02	<0.01
KC19744	650.71 ~ 651.19	<0.01	<0.01	<0.01	<0.01
KC19745	651.19 ~ 651.67	0.03	<0.01	<0.01	<0.01
KC19746	651.67 ~ 652.15	<0.01	<0.01	<0.01	<0.01
KC19747	652.15 ~ 652.63	<0.01	<0.01	<0.01	<0.01
KC19748	652.63 ~ 652.89	<0.01	<0.01	<0.01	<0.01

Width (m)	Depth (m)	T-Cu (%)	AS-Cu (%)	T-Co (%)
2.11	647.73 ~ 649.84	0.00	<0.02	0.00

MJZC-4

Sample No.	Depth (m)	T-Cu (%)	AS-Cu (%)	T-Co (%)	AS-Co (%)
KC15105	913.94 ~ 914.44	<0.01	<0.01	<0.01	<0.01
KC15106	914.44 ~ 914.94	<0.01	<0.01	<0.01	<0.01
KC15107	914.94 ~ 915.44	<0.01	<0.01	<0.01	<0.01
KC15108	915.44 ~ 915.94	<0.01	<0.01	<0.01	<0.01
KC15109	915.94 ~ 916.44	<0.01	<0.01	<0.01	<0.01
KC15110	916.44 ~ 916.94	<0.01	<0.01	<0.01	<0.01
KC15111	916.94 ~ 917.44	<0.01	<0.01	<0.01	<0.01
KC15112	917.44 ~ 917.94	<0.01	<0.01	<0.01	<0.01
KC15113	917.94 ~ 918.44	<0.01	<0.01	<0.01	<0.01
KC15114	918.44 ~ 918.94	<0.01	<0.01	<0.01	<0.01
KC15115	918.94 ~ 919.44	<0.01	<0.01	<0.01	<0.01
KC15116	919.44 ~ 919.94	<0.01	<0.01	<0.01	<0.01
KC15117	919.94 ~ 920.44	<0.01	<0.01	0.01	<0.01
KC15118	920.44 ~ 920.94	<0.01	<0.01	<0.01	<0.01
KC15119	920.94 ~ 921.44	<0.01	<0.01	<0.01	<0.01
KC15120	921.44 ~ 921.94	<0.01	<0.01	<0.01	<0.01
KC15121	921.94 ~ 922.44	<0.01	<0.01	<0.01	<0.01
KC15122	922.44 ~ 922.94	<0.01	<0.01	<0.01	<0.01
KC15123	922.94 ~ 923.44	<0.01	<0.01	<0.01	<0.01
KC15124	923.44 ~ 923.94	<0.01	<0.01	<0.01	<0.01
KC15125	923.94 ~ 924.44	<0.01	<0.01	<0.01	<0.01
KC15126	924.44 ~ 924.94	<0.01	<0.01	<0.01	<0.01
KC15127	924.94 ~ 925.19	<0.01	<0.01	<0.01	<0.01
KC15128	925.19 ~ 925.69	<0.01	<0.01	<0.01	<0.01
KC15129	925.69 ~ 926.19	<0.01	<0.01	<0.01	<0.01
KC15130	926.19 ~ 926.69	<0.01	<0.01	<0.01	<0.01
KC15131	926.69 ~ 927.19	<0.01	<0.01	<0.01	<0.01
KC15132	927.19 ~ 927.69	<0.01	<0.01	<0.01	<0.01
KC15133	927.69 ~ 928.19	<0.01	<0.01	<0.01	<0.01
KC15134	928.19 ~ 928.69	0.02	<0.01	<0.01	<0.01
KC15135	928.69 ~ 929.19	<0.01	<0.01	<0.01	<0.01
KC15136	929.19 ~ 929.69	0.02	<0.01	<0.01	<0.01
KC15137	929.69 ~ 930.14	0.03	<0.01	<0.01	<0.01
KC15138	930.14 ~ 930.64	0.07	<0.01	<0.01	<0.01
KC15139	930.64 ~ 931.14	0.21	<0.01	0.02	<0.01
KC15140	931.14 ~ 931.64	0.45	<0.01	<0.01	<0.01
KC15141	931.64 ~ 932.14	0.13	<0.01	<0.01	<0.01
KC15142	932.14 ~ 932.64	0.12	<0.01	<0.01	<0.01
KC15143	932.64 ~ 933.14	0.12	<0.01	<0.01	<0.01
KC15144	933.14 ~ 933.64	0.06	<0.01	<0.01	<0.01
KC15145	933.64 ~ 934.14	0.11	<0.01	<0.01	<0.01
KC15146	934.14 ~ 934.64	0.12	<0.01	<0.01	<0.01
KC15147	934.64 ~ 934.94	0.04	<0.01	<0.01	<0.01
KC15148	934.94 ~ 935.44	0.12	<0.01	<0.01	<0.01
KC15149	935.44 ~ 935.99	0.50	<0.01	<0.01	<0.01
KC15150	935.99 ~ 936.49	0.13	<0.01	0.02	<0.01
KC15151	936.49 ~ 936.99	0.15	<0.01	0.01	<0.01
KC15152	936.99 ~ 937.49	0.41	<0.01	0.02	<0.01
KC15153	937.49 ~ 937.99	0.15	<0.01	0.05	<0.01
KC15154	937.99 ~ 938.49	0.02	<0.01	0.02	<0.01
KC15155	938.49 ~ 938.99	0.01	<0.01	0.02	<0.01
KC15156	938.99 ~ 939.49	0.02	<0.01	0.02	<0.01
KC15157	939.49 ~ 939.99	<0.01	<0.01	0.01	<0.01
KC15158	939.99 ~ 940.49	<0.01	<0.01	0.01	<0.01
KC15159	940.49 ~ 940.94	<0.01	<0.01	0.01	<0.01

Table 2-5-1 Results of Chemical Analysis of Ore Samples (3)

MJZC-5

Sample (m)	Depth (m)	T-Cu (%)	AS-Cu (%)	T-Co (%)
LC14390	962.91 ~ 963.41	0.02	0.02	<0.01
LC14391	963.41 ~ 963.91	<0.01	<0.01	<0.01
LC14392	963.91 ~ 964.41	<0.01	<0.01	<0.01
LC14393	964.41 ~ 964.91	<0.01	<0.01	<0.01
LC14394	964.91 ~ 965.41	<0.01	<0.01	<0.01
LC14395	965.41 ~ 965.91	<0.01	<0.01	<0.01
LC14396	965.91 ~ 966.41	<0.01	<0.01	<0.01
LC14397	966.41 ~ 966.91	<0.01	<0.01	<0.01
LC14398	966.91 ~ 967.21	<0.01	<0.01	<0.01
LC14399	967.21 ~ 967.77	<0.01	<0.01	<0.01
LC14400	967.77 ~ 968.15	<0.01	<0.01	<0.01
LC18001	968.15 ~ 968.65	<0.01	<0.01	<0.01
LC18002	968.65 ~ 969.15	<0.01	<0.01	<0.01
LC18003	969.15 ~ 969.65	<0.01	<0.01	<0.01
LC18004	969.65 ~ 970.15	<0.01	<0.01	<0.01
LC18005	970.15 ~ 970.65	<0.01	<0.01	<0.01
LC18006	970.65 ~ 971.15	<0.01	<0.01	<0.01
LC18007	971.15 ~ 971.65	0.02	<0.01	<0.01
LC18008	971.65 ~ 972.15	0.05	<0.01	<0.01
LC18009	972.15 ~ 972.65	0.14	<0.01	<0.01
LC18010	972.65 ~ 973.15	1.01	<0.01	<0.01
LC18011	973.15 ~ 974.15	0.71	<0.01	0.03
LC18012	974.15 ~ 974.60	0.10	<0.01	0.02
LC18013	974.60 ~ 975.23	0.07	<0.01	0.02
LC18014	975.23 ~ 975.77	0.02	<0.01	0.02
LC18015	975.77 ~ 976.31	0.12	<0.01	0.01
LC18016	976.31 ~ 976.85	0.42	<0.01	0.01
LC18017	976.85 ~ 977.39	0.06	<0.01	0.02
LC18018	977.39 ~ 977.93	0.24	<0.01	0.01
LC18019	977.93 ~ 978.47	0.02	<0.01	0.02
LC18020	978.47 ~ 979.01	0.13	<0.01	0.02
LC18021	979.01 ~ 979.55	0.04	<0.01	0.04
LC18022	979.55 ~ 980.09	2.28	0.92	0.03
LC18023	980.09 ~ 980.15	0.37	<0.01	0.10
LC18024	980.15 ~ 980.65	1.25	1.25	0.02
LC18025	980.65 ~ 981.15	1.62	0.01	0.03
LC18026	981.15 ~ 981.65	2.39	0.02	0.04
LC18027	981.65 ~ 982.15	2.51	0.02	0.03
LC18028	982.15 ~ 982.65	1.80	0.02	0.03
LC18029	982.65 ~ 983.15	0.67	<0.01	0.03
LC18030	983.15 ~ 983.65	1.15	0.01	0.03
LC18031	983.65 ~ 984.15	0.12	<0.01	0.03
LC18032	984.15 ~ 984.65	0.02	<0.01	0.03
LC18033	984.65 ~ 985.15	0.03	<0.01	0.03
LC18034	985.15 ~ 985.31	0.65	<0.01	0.03
LC18035	985.31 ~ 985.84	1.08	0.01	0.04
LC18036	985.84 ~ 986.37	1.22	<0.01	0.02
LC18037	986.37 ~ 986.90	1.23	0.01	0.02
LC18038	986.90 ~ 987.43	0.73	<0.01	0.01
LC18039	987.43 ~ 987.96	0.13	<0.01	<0.01
LC18040	987.96 ~ 988.49	0.30	<0.01	<0.01
LC18041	988.49 ~ 989.02	0.14	<0.01	0.01
LC18042	989.02 ~ 989.55	0.09	<0.01	<0.01
LC18043	989.55 ~ 990.08	0.10	<0.01	0.01
LC18044	990.08 ~ 990.61	0.10	<0.01	<0.01
LC18045	990.61 ~ 991.14	0.08	<0.01	<0.01
LC18046	991.14 ~ 991.31	0.17	<0.01	<0.01
LC18047	991.31 ~ 991.81	0.09	<0.01	<0.01
LC18048	991.81 ~ 992.31	0.04	<0.01	<0.01
LC18049	992.31 ~ 992.81	0.07	<0.01	<0.01
LC18050	992.81 ~ 993.31	0.10	<0.01	<0.01
LC18051	993.31 ~ 993.81	0.06	<0.01	0.01
LC18052	993.81 ~ 994.31	0.05	<0.01	<0.01
LC18053	994.31 ~ 994.81	0.06	<0.01	<0.01
LC18054	994.81 ~ 995.31	0.05	<0.01	<0.01
LC18055	995.31 ~ 995.81	0.06	<0.01	0.01
LC18056	995.81 ~ 996.31	0.04	<0.01	<0.01
LC18057	996.31 ~ 996.81	0.06	<0.01	<0.01
LC18058	996.81 ~ 997.31	0.06	<0.01	<0.01
LC18059	997.31 ~ 997.81	0.05	<0.01	<0.01
LC18060	997.81 ~ 998.31	0.03	<0.01	<0.01
LC18061	998.31 ~ 998.81	0.16	<0.01	0.02
LC18062	998.81 ~ 999.17	0.09	<0.01	<0.01
LC18063	999.17 ~ 999.47	0.11	<0.01	0.01
LC18064	999.47 ~ 999.97	0.23	<0.01	0.01
LC18065	999.97 ~ 1000.47	0.56	<0.01	<0.01
LC18066	1000.47 ~ 1000.82	0.90	<0.01	<0.01
LC18067	1000.82 ~ 1001.12	2.74	<0.01	0.02
LC18068	1001.12 ~ 1001.47	1.61	<0.01	0.02
LC18069	1001.47 ~ 1001.97	2.19	<0.01	0.02
LC18070	1001.97 ~ 1002.47	1.99	<0.01	0.03
LC18071	1002.47 ~ 1003.45	2.66	<0.01	0.06
LC18072	1003.45 ~ 1003.96	0.47	<0.01	0.02
LC18073	1003.96 ~ 1004.23	0.87	<0.01	0.03
LC18074	1004.23 ~ 1004.73	2.00	<0.01	0.14
LC18075	1004.73 ~ 1005.03	0.42	<0.01	0.32
LC18076	1005.03 ~ 1005.13	0.06	<0.01	0.08
LC18077	1005.13 ~ 1005.68	0.06	<0.01	0.02
LC18078	1005.68 ~ 1006.23	0.06	<0.01	<0.01
LC18079	1006.23 ~ 1006.78	0.06	<0.01	<0.01
LC18080	1006.78 ~ 1007.33	0.06	<0.01	<0.01
LC18081	1007.33 ~ 1007.88	0.06	<0.01	<0.01
LC18082	1007.88 ~ 1008.43	0.07	<0.01	<0.01
LC18083	1008.43 ~ 1008.98	0.13	<0.01	<0.01
LC18084	1008.98 ~ 1009.13	0.07	<0.01	<0.01

Width (m)	Depth (m)	T-Cu (%)	AS-Cu (%)	T-Co (%)
3.1	979.55 ~ 982.65	1.93	0.02	0.03
7.88	979.55 ~ 987.43	1.13	0.01	0.03
2.64	1000.82 ~ 1003.45	2.32	<0.01	0.07
3.91	1000.82 ~ 1004.73	1.63	<0.01	0.04
4.76	999.97 ~ 1004.73	1.71	<0.01	0.04

MJZC-7

Sample No.	Depth (m)	T-Cu (%)	AS-Cu (%)	T-Co (%)
LC15917	918.96 ~ 919.46	<0.01	<0.01	<0.01
LC15918	919.46 ~ 919.96	<0.01	<0.01	<0.01
LC15919	919.96 ~ 920.46	<0.01	<0.01	<0.01
LC15920	920.46 ~ 920.96	<0.01	<0.01	<0.01
LC15921	920.96 ~ 921.46	<0.01	<0.01	<0.01
LC15922	921.46 ~ 921.96	<0.01	<0.01	<0.01
LC15923	921.96 ~ 922.46	<0.01	<0.01	<0.01
LC15924	922.46 ~ 922.96	0.12	<0.01	<0.01
LC15925	922.96 ~ 923.46	0.19	<0.01	<0.01
LC15926	923.46 ~ 923.89	0.43	<0.01	<0.01
LC15927	923.89 ~ 924.19	0.17	<0.01	0.01
LC15928	924.19 ~ 924.69	0.24	<0.01	<0.01
LC15929	924.69 ~ 924.96	0.23	<0.01	<0.01
LC15930	924.96 ~ 925.46	0.10	<0.01	<0.01
LC15931	925.46 ~ 925.96	0.05	<0.01	<0.01
LC15932	925.96 ~ 926.46	0.04	<0.01	<0.01
LC15933	926.46 ~ 926.96	0.12	<0.01	<0.01
LC15934	926.96 ~ 927.46	0.13	<0.01	<0.01
LC15935	927.46 ~ 927.96	0.09	<0.01	<0.01
LC15936	927.96 ~ 928.46	0.09	<0.01	<0.01
LC15937	928.46 ~ 928.96	0.13	<0.01	<0.01
LC15938	928.96 ~ 929.46	0.08	<0.01	<0.01
LC15939	929.46 ~ 929.96	0.10	<0.01	<0.01
LC15940	929.96 ~ 930.46	0.04	<0.01	<0.01
LC15941	930.46 ~ 930.58	0.04	<0.01	<0.01
LC15942	930.58 ~ 931.08	0.06	<0.01	<0.01
LC15943	931.08 ~ 931.58	0.07	<0.01	<0.01
LC15944	931.58 ~ 932.08	0.06	<0.01	<0.01
LC15945	932.08 ~ 932.58	0.10	<0.01	<0.01
LC15946	932.58 ~ 933.08	0.07	<0.01	<0.01
LC15947	933.08 ~ 933.58	0.04	<0.01	<0.01
LC15948	933.58 ~ 933.88	0.12	<0.01	<0.01
LC15949	933.88 ~ 934.18	0.02	<0.01	<0.01
LC15950	934.18 ~ 934.49	0.15	<0.01	<0.01
LC15951	934.49 ~ 934.98	0.09	<0.01	<0.01
LC15952	934.98 ~ 935.48	0.12	<0.01	<0.01
LC15953	935.48 ~ 935.98	<0.01	<0.01	<0.01
LC15954	935.98 ~ 936.48	<0.01	<0.01	<0.01
LC15955	936.48 ~ 936.64	<0.01	<0.01	<0.01
LC15956	936.64 ~ 937.14	<0.01	<0.01	<0.01
LC15957	937.14 ~ 937.64	<0.01	<0.01	<0.01
LC15958	937.64 ~ 937.94	<0.01	<0.01	<0.01
LC15959	937.94 ~ 938.44	<0.01	<0.01	<0.01
LC15960	938.44 ~ 938.94	<0.01	<0.01	<0.01
LC15961	938.94 ~ 939.44	<0.01	<0.01	<0.01
LC15962	939.44 ~ 939.94	<0.01	<0.01	<0.01
LC15963	939.94 ~ 940.44	<0.01	<0.01	<0.01
LC15964	940.44 ~ 940.94	<0.01	<0.01	<0.01
LC15965	940.94 ~ 941.44	0.01	<0.01	<0.01
LC15966	941.44 ~ 941.94	0.03	<0.01	<0.01
LC15967	941.94 ~ 942.44	<0.01	<0.01	<0.01
LC15968	942.44 ~ 942.73	<0.01	<0.01	<0.01
LC15969	942.73 ~ 943.23	<0.01	<0.01	<0.01
LC15970	943.23 ~ 943.73	0.02	<0.01	<0.01
LC15971	943.73 ~ 944.23	0.02	<0.01	<0.01
LC15972	944.23 ~ 944.73	0.03	<0.01	<0.01
LC15973	944.73 ~ 945.23	0.02	<0.01	<0.01
LC15974	945.23 ~ 945.73	<0.01	<0.01	<0.01
LC15975	945.73 ~ 946.23	<0.01	<0.01	<0.01
LC15976	946.23 ~ 946.73	<0.01	<0.01	<0.01
LC15977	946.73 ~ 947.23	<0.01	<0.01	<0.01
LC15978	947.23 ~ 947.73	<0.01	<0.01	<0.01
LC15979	947.73 ~ 948.45	0.14	<0.01	0.04
LC15980	948.45 ~ 948.78	1.30	<0.01	0.02
LC15981	948.78 ~ 949.08	1.81	<0.01	0.02
LC15982	949.08 ~ 949.58	1.90	<0.01	0.04
LC15983	949.58 ~ 949.75	0.61	<0.01	0.01
LC15984	949.75 ~ 950.06	1.45	<0.01	0.02
LC15985	950.06 ~ 950.56	2.42	<0.01	0.03
LC15986	950.56 ~ 951.06	2.14	<0.01	0.02
LC15987	951.06 ~ 951.13	0.55	<0.01	<0.01
LC15988	951.13 ~ 951.43	1.81	<0.01	0.02
LC15989	951.43 ~ 951.93	0.57	<0.01	<0.01
LC15990	951.93 ~ 952.43	0.46	<0.01	<0.01
LC15991	952.43 ~ 952.93	0.75	<0.01	<0.01
LC15992	952.93 ~ 953.33	1.20	<0.01	0.01
LC15993	953.33 ~ 953.63	0.70	<0.01	<0.01
LC15994	953.63 ~ 954.15	0.96	<0.01	<0.01
LC15995	954.15 ~ 954.67	1.32	<0.01	<0.01
LC15996	954.67 ~ 954.98	0.47	<0.01	<0.01
LC15997	954.98 ~ 955.48	0.82	<0.01	<0.01
LC15998	955.48 ~ 956.00	0.36	<0.01	<0.01
LC15999	956.00 ~ 956.52	0.51	<0.01	0.01
LC16000	956.52 ~ 957.04	0.28	<0.01	<0.01
LC14301	957.04 ~ 957.56	0.11	<0.01	<0.01
LC14302	957.56 ~ 958.08	0.41	<0.01	<0.01
LC14303	958.08 ~ 958.60	0.60	<0.01	<0.01
LC14304	958.60 ~ 959.12	0.14	<0.01	<0.01
LC14305	959.12 ~ 959.64	0.57	<0.01	<0.01
LC14306	959.64 ~ 960.16	0.10	<0.01	<0.01
LC14307	960.16 ~ 960.56	0.17	<0.01	<0.01
LC14308	960.56 ~ 961.11	0.03	<0.01	<0.01
LC14309	961.11 ~ 961.66	<0.01	<0.01	<0.01
LC14310	961.66 ~ 962.06	<0.01	<0.01	<0.01
LC14311	962.06 ~ 962.39	0.26	<0.01	<0.01
LC14312	962.39 ~ 962.84	0.06	<0.01	<0.01
LC14313	962.84 ~ 963.39	0.28	<0.01	<0.01
LC14314	963.39 ~ 963.84	0.02	<0.01	<0.01
LC14315	963.84 ~ 964.39	<0.01	<0.01	<0.01
LC14316	964.39 ~ 965.09	<0.01	<0.01	<0.01
LC14317	965.09 ~ 965.39	<0.01	<0.01	<0.01
LC14318	965.39 ~ 965.84	<0.01	<0.01	<0.01
LC14319	965.84 ~ 966.39	<0.01	<0.01	<0.01
LC14320	966.39 ~ 966.96	<0.01	<0.01	<0.01

Width (m)	Depth (m)	T-Cu (%)	AS-Cu (%)	T-Co (%)
2.99	948.45 ~ 951.43	1.78	<0.01	0.02
8.07	948.45 ~ 956.52	1.13	<0.01	0.01

Table 2-5-1 Results of Chemical Analysis of Ore Samples (4)

MJZC－6

Sample (m)	Depth (m)	T-Cu (%)	AS-Cu (%)	T-Co (%)
LC19794	873.77 ~ 874.38	0.51	0.01	<0.01
LC19795	874.38 ~ 874.73	0.47	0.02	0.01
LC19796	874.73 ~ 875.23	0.18	0.03	0.01
LC19797	875.23 ~ 875.73	0.01	0.01	0.01
LC19798	875.73 ~ 876.23	0.01	<0.01	0.01
LC19799	876.23 ~ 876.73	0.03	<0.01	0.01
LC19800	876.73 ~ 877.23	0.01	<0.01	<0.01
LC14201	877.23 ~ 877.60	0.19	0.03	0.03
LC14202	877.60 ~ 878.05	0.07	0.04	<0.01
LC14203	955.15 ~ 955.65	<0.01	<0.01	<0.01
LC14204	955.65 ~ 956.15	0.01	<0.01	<0.01
LC14205	956.15 ~ 956.65	0.02	0.01	<0.01
LC14206	956.65 ~ 957.15	<0.01	<0.01	<0.01
LC14207	957.15 ~ 957.65	0.04	0.02	<0.01
LC14208	957.65 ~ 958.15	0.05	0.02	<0.01
LC14209	958.15 ~ 958.65	0.01	0.01	<0.01
LC14210	958.65 ~ 959.15	0.12	0.01	<0.01
LC14211	959.15 ~ 959.35	0.10	0.01	<0.01
LC14212	959.35 ~ 959.73	1.84	0.04	<0.01
LC14213	959.73 ~ 961.15	0.02	<0.01	<0.01
LC14214	961.15 ~ 961.65	<0.01	<0.01	<0.01
LC14215	961.65 ~ 962.15	<0.01	<0.01	<0.01
LC14216	962.15 ~ 962.65	<0.01	<0.01	<0.01
LC14217	962.65 ~ 963.15	<0.01	<0.01	<0.01
LC14218	963.15 ~ 963.65	<0.01	<0.01	<0.01
LC14219	963.65 ~ 964.15	<0.01	<0.01	<0.01
LC14220	964.15 ~ 964.65	<0.01	<0.01	<0.01
LC14221	964.65 ~ 965.15	0.13	<0.01	<0.01
LC14222	965.15 ~ 965.65	0.38	<0.01	<0.01
LC14223	965.65 ~ 966.15	<0.01	<0.01	<0.01
LC14224	966.15 ~ 966.65	0.01	<0.01	<0.01
LC14225	966.65 ~ 966.95	0.01	<0.01	<0.01
LC14226	966.95 ~ 967.45	<0.01	<0.01	<0.01
LC14227	967.45 ~ 967.95	<0.01	<0.01	<0.01
LC14228	967.95 ~ 968.45	<0.01	<0.01	<0.01
LC14229	968.45 ~ 968.95	0.04	<0.01	<0.01
LC14230	968.95 ~ 969.45	<0.01	<0.01	<0.01
LC14231	969.45 ~ 969.56	<0.01	<0.01	0.01
LC14232	969.56 ~ 970.06		<0.01	<0.01
LC14233	970.06 ~ 970.56	0.01	<0.01	<0.01
LC14234	970.56 ~ 971.06	<0.01	<0.01	<0.01
LC14235	971.06 ~ 971.56		<0.01	<0.01
LC14236	971.56 ~ 972.06		<0.01	<0.01
LC14237	972.06 ~ 972.56	0.04	<0.01	<0.01
LC14238	972.56 ~ 972.96	0.04	0.01	<0.01
LC14239	972.96 ~ 973.46	0.07	0.01	0.01
LC14240	973.46 ~ 973.76	0.08	0.01	<0.01
LC14241	973.76 ~ 974.06	0.08	<0.01	<0.01
LC14242	974.06 ~ 974.36	0.26	<0.01	<0.01
LC14243	974.36 ~ 974.86	0.29	<0.01	<0.01
LC14244	974.86 ~ 975.36	0.21	<0.01	<0.01
LC14245	975.36 ~ 975.86	0.27	<0.01	<0.01
LC14246	975.86 ~ 976.36	0.41	<0.01	<0.01
LC14247	976.36 ~ 976.86	0.22	<0.01	<0.01
LC14248	976.86 ~ 977.36	0.62	<0.01	<0.01
LC14249	977.36 ~ 977.86	0.63	<0.01	<0.01
LC14250	977.86 ~ 978.16	0.52	<0.01	<0.01
LC14251	978.16 ~ 978.46	0.14	<0.01	<0.01
LC14252	978.46 ~ 978.95	0.12	<0.01	<0.01
LC14253	978.95 ~ 979.45	0.43	<0.01	0.01
LC14254	979.45 ~ 979.95	0.16	<0.01	0.01
LC14255	979.95 ~ 980.45	0.22	<0.01	<0.01
LC14256	980.45 ~ 980.95	0.47	<0.01	0.01
LC14257	980.95 ~ 981.10	0.31	<0.01	<0.01
LC14258	981.10 ~ 981.40	0.54	0.02	<0.01
LC14259	981.40 ~ 981.90	1.22	<0.01	<0.01
LC14260	981.90 ~ 982.40	1.13	0.02	<0.01
LC14261	982.40 ~ 982.90	1.46	<0.01	<0.01
LC14262	982.90 ~ 983.40	1.57	<0.01	0.02
LC14263	983.40 ~ 983.95	1.02	<0.01	<0.01
LC14264	983.95 ~ 984.45	0.84	<0.01	<0.01
LC14265	984.45 ~ 984.96	0.44	<0.01	<0.01
LC14266	984.96 ~ 985.46	0.29	<0.01	<0.01
LC14267	985.46 ~ 985.85	0.67	<0.01	0.01
LC14268	985.85 ~ 986.35	0.16	<0.01	<0.01
LC14269	986.35 ~ 986.85	0.05	<0.01	<0.01
LC14270	986.85 ~ 987.35	0.06	<0.01	<0.01
LC14271	987.35 ~ 987.85	0.21	<0.01	<0.01
LC14272	987.85 ~ 988.35	0.16	<0.01	<0.01

Sample (m)	Depth (m)	T-Cu (%)	AS-Cu (%)	T-Co (%)
LC14273	0.00 ~ 0.50	0.52	<0.01	<0.01
LC14274	988.85 ~ 989.53	0.10	<0.01	<0.01
LC14275	989.53 ~ 990.03	0.25	<0.01	<0.01
LC14276	990.03 ~ 990.53	0.16	<0.01	<0.01
LC14277	990.53 ~ 990.96	0.11	<0.01	<0.01
LC14278	990.96 ~ 991.46	0.42	<0.01	<0.01
LC14279	991.46 ~ 991.96	0.29	<0.01	<0.01
LC14280	991.96 ~ 992.46	0.32	<0.01	<0.01
LC14281	992.46 ~ 992.79	0.32	<0.01	<0.01
LC14282	992.79 ~ 993.29	0.38	<0.01	<0.01
LC14283	993.29 ~ 993.79	0.17	<0.01	<0.01
LC14284	993.79 ~ 994.29	0.41	<0.01	<0.01
LC14285	994.29 ~ 994.79	0.50	<0.01	<0.01
LC14286	994.79 ~ 995.00	0.58	0.01	0.02
LC14287	995.00 ~ 995.68	1.28	<0.01	0.01
LC14288	995.68 ~ 996.18	0.40	<0.01	<0.01
LC14289	996.18 ~ 996.68	0.05	<0.01	<0.01
LC14290	996.68 ~ 996.96	0.75	0.01	<0.01
LC14291	996.96 ~ 997.46	0.61	0.01	<0.01
LC14292	997.46 ~ 997.96	0.03	<0.01	<0.01
LC14293	997.96 ~ 998.46	0.05	<0.01	<0.01
LC14294	998.46 ~ 998.96	0.02	<0.01	<0.01
LC14295	998.96 ~ 999.46	0.15	<0.01	<0.01
LC14296	999.46 ~ 999.96	0.03	<0.01	<0.01
LC14297	999.96 ~ 1000.46	0.11	<0.01	<0.01
LC14298	1000.46 ~ 1001.05	0.02	<0.01	<0.01
LC14299	1001.05 ~ 1001.55	0.27	<0.01	0.02
LC14300	1001.55 ~ 1002.05	0.10	<0.01	0.01
LC15901	1002.05 ~ 1002.55	0.04	<0.01	0.02
LC15902	1002.55 ~ 1002.96	0.08	<0.01	0.01
LC15903	1002.96 ~ 1003.10	0.10	<0.01	0.01
LC15904	1003.10 ~ 1003.60	0.13	<0.01	<0.01
LC15905	1003.60 ~ 1004.10	0.19	<0.01	<0.01
LC15906	1004.10 ~ 1004.60	0.19	<0.01	<0.01
LC15907	1004.60 ~ 1005.10	0.08	<0.01	<0.01
LC15908	1005.10 ~ 1005.60	0.08	<0.01	<0.01
LC15909	1005.60 ~ 1006.10	0.18	<0.01	<0.01
LC15910	1006.10 ~ 1006.43	0.21	<0.01	<0.01
LC15911	1006.43 ~ 1006.93	0.15	<0.01	0.01
LC15912	1006.93 ~ 1007.35	0.11	<0.01	0.01
LC15913	1007.35 ~ 1007.85	0.02	<0.01	<0.01
LC15914	1007.85 ~ 1008.35	0.01	<0.01	<0.01
LC15915	1008.35 ~ 1008.96	<0.01	<0.01	<0.01

Width (m)	Depth (m)	T-Cu (%)	AS-Cu (%)	T-Co (%)
3.35	981.10 ~ 984.45	1.14	<0.01	<0.01
1.39	994.29 ~ 995.68	0.89	<0.01	0.01

Table 2-5-1 Results of Chemical Analysis of Ore Samples (5)

MJZC-9

Sample No	Depth (m)	T-Cu (%)	AS-Cu (%)	T-Co (%)
KC12701	1077.45 ~ 1077.96	0.02	<0.01	<0.01
KC12702	1077.96 ~ 1078.45	<0.01	<0.01	<0.01
KC12703	1078.45 ~ 1079.00	<0.01	<0.01	0.01
KC12704	1079.00 ~ 1079.50	<0.01	<0.01	0.01
KC12705	1079.50 ~ 1079.67	0.06	<0.01	<0.01
KC12706	1079.67 ~ 1080.17	0.05	<0.01	<0.01
KC12707	1080.17 ~ 1080.67	0.09	<0.01	<0.01
KC12708	1080.67 ~ 1081.17	0.06	<0.01	<0.01
KC12709	1081.17 ~ 1081.67	0.06	<0.01	<0.01
KC12710	1081.67 ~ 1082.17	0.17	<0.01	<0.01
KC12711	1082.17 ~ 1082.67	0.17	<0.01	0.01
KC12712	1082.67 ~ 1083.17	0.15	<0.01	<0.01
KC12713	1083.17 ~ 1083.67	0.15	<0.01	0.01
KC12714	1083.67 ~ 1084.27	0.22	<0.01	<0.01
KC12715	1084.27 ~ 1084.68	0.92	<0.01	0.01
KC12716	1084.68 ~ 1085.18	0.45	<0.01	0.01
KC12717	1085.18 ~ 1085.68	0.52	<0.01	<0.01
KC12718	1085.68 ~ 1086.18	1.45	<0.01	<0.01
KC12719	1086.18 ~ 1086.68	2.44	<0.01	0.01
KC12720	1086.68 ~ 1087.18	2.58	0.01	0.01
KC12721	1087.18 ~ 1087.75	2.59	0.01	0.01
KC12722	1087.76 ~ 1088.26	2.35	<0.01	0.01
KC12723	1088.25 ~ 1088.75	0.18	<0.01	0.02
KC12724	1088.76 ~ 1089.25	0.70	<0.01	0.01
KC12725	1089.26 ~ 1089.50	1.53	<0.01	<0.01
KC12726	1089.50 ~ 1090.00	0.02	<0.01	0.02
KC12727	1090.00 ~ 1090.50	0.19	<0.01	0.02
KC12728	1090.50 ~ 1091.00	0.79	0.01	0.03
KC12729	1091.00 ~ 1091.50	0.69	0.01	0.02
KC12730	1091.50 ~ 1092.00	0.33	<0.01	0.02
KC12731	1092.00 ~ 1092.50	0.03	<0.01	0.03
KC12732	1092.50 ~ 1093.00	0.02	<0.01	0.02
KC12733	1093.00 ~ 1093.50	0.01	<0.01	0.02
KC12734	1093.50 ~ 1094.00	0.02	<0.01	0.02
KC12735	1094.00 ~ 1094.50	0.02	<0.01	0.02
KC12736	1094.50 ~ 1095.00	0.01	<0.01	0.02
KC12737	1095.00 ~ 1095.35	0.05	<0.01	0.02
KC12738	1095.35 ~ 1095.85	0.20	<0.01	0.03
KC12739	1095.85 ~ 1096.35	0.23	<0.01	0.03
KC12740	1096.35 ~ 1096.85	0.21	<0.01	0.01
KC12741	1096.85 ~ 1097.35	0.25	<0.01	0.01
KC12742	1097.35 ~ 1097.85	0.20	<0.01	0.02
KC12743	1097.85 ~ 1098.35	0.26	<0.01	0.02
KC12744	1098.35 ~ 1098.85	0.02	<0.01	0.02
KC12745	1098.85 ~ 1099.35	0.27	<0.01	0.02
KC12746	1099.35 ~ 1099.85	0.05	<0.01	0.03
KC12747	1099.85 ~ 1100.35	0.39	<0.01	0.02
KC12748	1100.35 ~ 1100.85	0.42	<0.01	0.01
KC12749	1100.85 ~ 1101.35	0.01	<0.01	0.02
KC12750	1101.35 ~ 1101.85	0.01	<0.01	0.02
KC12751	1101.85 ~ 1102.35	0.01	<0.01	0.02
KC12752	1102.35 ~ 1102.85	0.01	<0.01	0.03
KC12753	1102.85 ~ 1103.35	0.01	<0.01	0.03
KC12754	1103.35 ~ 1103.85	0.01	<0.01	0.04
KC12755	1103.85 ~ 1104.35	0.01	<0.01	0.05
KC12756	1104.35 ~ 1104.85	0.41	<0.01	0.05
KC12757	1104.85 ~ 1105.35	0.06	<0.01	0.09
KC12758	1105.35 ~ 1105.76	0.06	<0.01	0.07
KC12759	1105.76 ~ 1106.26	0.07	<0.01	<0.01
KC12760	1106.26 ~ 1106.75	0.07	<0.01	0.05
KC12761	1106.76 ~ 1107.26	0.05	<0.01	0.05
KC12762	1107.25 ~ 1107.76	0.11	<0.01	0.04
KC12763	1107.76 ~ 1108.15	0.03	<0.01	0.04
KC12764	1108.16 ~ 1108.36	0.80	<0.01	0.05
KC12765	1108.35 ~ 1108.85	2.65	<0.01	0.02
KC12766	1108.85 ~ 1109.36	1.99	<0.01	0.01
KC12767	1109.35 ~ 1109.86	2.68	<0.01	0.02
KC12768	1109.86 ~ 1110.36	1.99	0.01	0.02
KC12769	1110.36 ~ 1110.86	3.23	<0.01	0.07
KC12770	1110.86 ~ 1111.36	3.15	0.01	0.03
KC12771	1111.36 ~ 1111.76	4.47	<0.01	0.04
KC12772	1111.76 ~ 1112.26	3.59	0.01	0.25
KC12773	1112.26 ~ 1112.76	1.88	0.01	0.31
KC12774	1112.76 ~ 1113.26	1.97	0.01	0.04
KC12775	1113.26 ~ 1113.76	2.57	<0.01	0.14
KC12776	1113.76 ~ 1114.26	1.98	<0.01	0.02
KC12777	1114.26 ~ 1114.76	0.77	<0.01	0.01
KC12778	1114.76 ~ 1115.26	0.87	<0.01	0.02
KC12779	1115.26 ~ 1115.76	0.75	<0.01	0.01
KC12780	1115.76 ~ 1115.26	0.70	<0.01	0.01

Sample No	Depth (m)	T-Cu (%)	AS-Cu (%)	T-Co (%)
KC12781	1115.25 ~ 1115.76	0.38	<0.01	<0.01
KC12782	1116.76 ~ 1117.00	0.48	<0.01	<0.01
KC12783	1117.00 ~ 1117.50	1.06	<0.01	<0.01
KC12784	1117.50 ~ 1118.00	1.47	<0.01	<0.01
KC12785	1118.00 ~ 1118.50	0.82	<0.01	0.01
KC12786	1118.50 ~ 1119.00	0.33	<0.01	0.01
KC12787	1119.00 ~ 1119.50	0.37	<0.01	<0.01
KC12788	1119.50 ~ 1120.00	1.03	<0.01	0.06
KC12789	1120.00 ~ 1120.50	0.73	<0.01	0.03
KC12790	1120.50 ~ 1120.75	0.32	<0.01	0.01
KC12791	1120.76 ~ 1121.25	0.41	<0.01	0.01
KC12792	1121.25 ~ 1121.75	0.10	<0.01	<0.01
KC12793	1121.75 ~ 1122.25	0.04	<0.01	<0.01
KC12794	1122.25 ~ 1122.76	0.04	<0.01	0.01
KC12795	1122.76 ~ 1123.25	0.02	<0.01	<0.01
KC12796	1123.25 ~ 1123.75	0.07	<0.01	<0.01
KC12797	1123.76 ~ 1124.25	0.03	<0.01	0.01
KC12798	1124.26 ~ 1124.75	0.01	<0.01	0.01
KC12799	1124.75 ~ 1125.26	0.01	<0.01	0.01
KC12800	1125.26 ~ 1125.75	0.03	<0.01	0.01
KC15101	1125.75 ~ 1125.26	0.01	<0.01	0.01
KC15102	1125.26 ~ 1125.75	0.02	<0.01	0.01

Width (m)	Depth (m)	T-Cu (%)	AS-Cu (%)	T-Co (%)
2.58	1085.68 ~ 1088.26	2.29	<0.01	<0.01
5.90	1108.35 ~ 1114.26	3.12	<0.01	0.08
6.24	1114.26 ~ 1120.50	0.78	<0.01	<0.02

Table 2-5-1 Results of Chemical Analysis of Ore Samples (6)

MJZC-10

Sample No	Depth (m)	T-Cu (%)	As-Cu (%)	T-Co (%)
KC12222	953.70 ~ 954.70	0.01	<0.01	0.01
KC12223	954.70 ~ 955.70	<0.01	<0.01	<0.01
KC12224	955.70 ~ 956.70	0.01	<0.01	<0.01
KC12225	956.70 ~ 957.70	<0.01	<0.01	<0.01
KC12226	957.70 ~ 958.70	<0.01	<0.01	<0.01
KC12227	958.70 ~ 959.70	<0.01	<0.01	<0.01
KC12228	959.70 ~ 960.70	<0.01	<0.01	<0.01
KC12229	960.70 ~ 961.33	<0.01	<0.01	<0.01
KC12230	961.33 ~ 961.83	<0.01	<0.01	<0.01
KC12231	961.83 ~ 962.33	<0.01	<0.01	<0.01
KC12232	962.33 ~ 962.70	<0.01	<0.01	<0.01
KC12233	962.70 ~ 963.20	<0.01	<0.01	<0.01
KC12234	963.20 ~ 963.70	0.01	<0.01	<0.01
KC12235	963.70 ~ 964.20	<0.01	<0.01	<0.01
KC12236	964.20 ~ 964.70	0.01	<0.01	<0.01
KC12237	964.70 ~ 965.20	0.03	<0.01	0.01
KC12238	965.20 ~ 965.70	<0.01	<0.01	0.02
KC12239	965.70 ~ 966.20	<0.01	<0.01	0.01
KC12240	966.20 ~ 966.70	<0.01	<0.01	0.01
KC12241	966.70 ~ 967.20	<0.01	<0.01	0.01
KC12242	967.20 ~ 967.70	<0.01	<0.01	0.01
KC12243	967.70 ~ 968.20	0.01	<0.01	0.01
KC12244	968.20 ~ 968.70	<0.01	<0.01	<0.01
KC12245	968.70 ~ 969.20	0.01	<0.01	0.01
KC12246	969.20 ~ 969.70	<0.01	<0.01	<0.01
KC12247	969.70 ~ 970.20	<0.01	<0.01	<0.01
KC12248	970.20 ~ 970.70	0.07	<0.01	<0.01
KC12249	970.70 ~ 971.20	0.01	<0.01	<0.01
KC12250	971.20 ~ 971.70	<0.01	<0.01	0.01
KC12251	971.70 ~ 972.20	0.01	<0.01	0.01
KC12252	972.20 ~ 972.70	<0.01	<0.01	0.01
KC12253	972.70 ~ 973.20	0.01	<0.01	0.01
KC12254	973.20 ~ 973.62	0.02	<0.01	0.01
KC12255	973.62 ~ 974.12	0.03	<0.01	0.03
KC12256	974.12 ~ 974.62	0.03	<0.01	0.03
KC12257	974.62 ~ 975.12	0.18	<0.01	0.03
KC12258	975.12 ~ 975.62	0.22	<0.01	0.04
KC12259	975.62 ~ 976.16	0.08	<0.01	0.02
KC12260	976.16 ~ 976.66	0.11	<0.01	0.02
KC12261	976.66 ~ 977.16	0.23	<0.01	0.02
KC12262	977.16 ~ 977.66	0.32	<0.01	<0.01
KC12263	977.66 ~ 978.16	0.12	<0.01	0.01
KC12264	978.16 ~ 978.66	0.10	<0.01	0.01
KC12265	978.66 ~ 979.16	0.12	<0.01	0.01
KC12266	979.16 ~ 979.66	0.05	<0.01	0.01
KC12267	979.66 ~ 980.16	0.05	<0.01	0.01
KC12268	980.16 ~ 980.70	0.05	<0.01	0.01
KC12269	980.70 ~ 981.20	0.06	<0.01	0.01
KC12270	981.20 ~ 981.70	0.08	<0.01	0.01
KC12271	981.70 ~ 982.20	0.11	<0.01	0.02
KC12272	982.20 ~ 982.70	1.77	<0.01	0.04
KC12273	982.70 ~ 983.20	1.52	<0.01	0.03
KC12274	983.20 ~ 983.70	0.80	<0.01	0.03
KC12275	983.70 ~ 984.20	0.23	<0.01	0.04
KC12276	984.20 ~ 984.70	<0.01	<0.01	0.03
KC12277	984.70 ~ 985.20	0.15	<0.01	<0.01
KC12278	985.20 ~ 985.70	0.05	<0.01	0.04
KC12279	985.70 ~ 986.20	0.05	<0.01	0.07
KC12280	986.20 ~ 986.70	0.79	<0.01	0.03
KC12281	986.70 ~ 987.20	0.11	<0.01	0.02
KC12282	987.20 ~ 987.56	0.34	<0.01	0.02
KC12283	987.56 ~ 988.06	0.29	0.01	<0.01
KC12284	988.06 ~ 988.56	0.54	0.01	<0.01
KC12285	988.56 ~ 989.06	0.47	0.01	<0.01
KC12286	989.06 ~ 989.70	0.24	<0.01	<0.01
KC12287	989.70 ~ 990.20	0.21	<0.01	<0.01
KC12288	990.20 ~ 990.70	0.39	<0.01	<0.01
KC12289	990.70 ~ 991.20	0.25	0.01	<0.01
KC12290	991.20 ~ 991.88	0.05	<0.01	<0.01
KC12291	991.88 ~ 992.38	0.25	<0.01	<0.01
KC12292	992.38 ~ 992.88	0.22	0.01	<0.01
KC12293	992.88 ~ 993.56	0.41	0.03	<0.01
KC12294	993.56 ~ 994.06	0.34	0.01	<0.01
KC12295	994.06 ~ 994.56	0.32	<0.01	<0.01
KC12296	994.56 ~ 995.06	0.35	<0.01	<0.01
KC12297	995.06 ~ 995.56	0.19	0.01	<0.01
KC12298	995.56 ~ 996.06	0.18	0.08	<0.01
KC12299	996.06 ~ 996.56	0.10	0.01	<0.01
KC12300	996.56 ~ 997.06	0.09	0.02	<0.01
KC18932	997.06 ~ 997.56	0.09	<0.01	<0.01

Width (m)	Depth (m)	As-Cu (%)	T-Co (%)
1.00	982.20 ~ 983.20	<0.01	0.04

MJZC-11

Sample No	Depth (m)	T-Cu (%)	As-Cu (%)	T-Co (%)
KC16103	635.05 ~ 635.55	<0.01	<0.01	<0.01
KC16104	635.55 ~ 636.05	<0.01	<0.01	0.01
KC16105	636.05 ~ 636.55	<0.01	<0.01	0.01
KC16106	636.55 ~ 637.05	<0.01	<0.01	<0.01
KC16107	637.05 ~ 637.55	<0.01	<0.01	0.01
KC16108	637.55 ~ 638.05	<0.01	<0.01	0.02
KC16109	638.05 ~ 638.55	<0.01	<0.01	0.05
KC16110	638.55 ~ 639.05	<0.01	<0.01	0.03
KC16111	639.05 ~ 639.55	<0.01	<0.01	0.02
KC16112	639.55 ~ 640.05	<0.01	<0.01	0.02
KC16113	640.05 ~ 640.55	<0.01	<0.01	0.02
KC16114	640.55 ~ 641.05	0.01	<0.01	0.02
KC16115	641.05 ~ 641.55	<0.01	<0.01	0.02
KC16116	641.55 ~ 642.05	<0.01	<0.01	0.02
KC16117	642.05 ~ 642.55	<0.01	<0.01	0.03
KC16118	642.55 ~ 642.75	<0.01	<0.01	0.02
KC16119	642.75 ~ 643.25	0.02	<0.01	0.06
KC16120	643.25 ~ 643.75	0.02	<0.01	0.14
KC16121	643.75 ~ 644.25	0.01	<0.01	0.07
KC16122	644.25 ~ 644.75	0.01	<0.01	0.03
KC16123	644.75 ~ 645.25	0.02	<0.01	0.02
KC16124	645.25 ~ 645.75	0.01	<0.01	0.02
KC16125	645.75 ~ 646.25	0.06	<0.01	0.02
KC16126	646.25 ~ 646.75	0.08	<0.01	0.02
KC16127	646.75 ~ 647.05	0.18	<0.01	0.02
KC16128	647.05 ~ 647.55	0.28	<0.01	0.02
KC16129	647.55 ~ 648.05	0.53	<0.01	0.02
KC16130	648.05 ~ 648.55	0.26	<0.01	0.01
KC16131	648.55 ~ 649.05	0.21	<0.01	0.01
KC16132	649.05 ~ 649.55	0.33	<0.01	0.01
KC16133	649.55 ~ 650.05	0.21	<0.01	0.02
KC16134	650.05 ~ 650.55	0.27	<0.01	0.01
KC16135	650.55 ~ 651.05	0.49	0.01	0.02
KC16136	651.05 ~ 651.55	0.40	0.01	0.02
KC16137	651.55 ~ 652.05	0.13	<0.01	0.01
KC16138	652.05 ~ 652.55	0.13	<0.01	0.01
KC16139	652.55 ~ 653.05	0.24	<0.01	0.02
KC16140	653.05 ~ 653.35	0.17	<0.01	0.01
KC16141	653.35 ~ 653.85	0.22	<0.01	0.02
KC16142	653.85 ~ 654.35	0.44	0.01	0.02
KC16143	654.35 ~ 654.85	1.85	<0.01	0.04
KC16144	654.85 ~ 655.30	1.55	<0.01	0.06
KC16145	655.30 ~ 655.80	0.57	<0.01	0.07
KC16146	655.80 ~ 656.30	0.24	<0.01	0.07
KC16147	656.30 ~ 656.70	0.70	<0.01	0.06
KC16148	656.70 ~ 657.20	<0.01	<0.01	<0.01
KC16149	657.20 ~ 657.70	<0.01	<0.01	<0.01
KC16150	657.70 ~ 658.20	<0.01	<0.01	<0.01
KC16151	658.20 ~ 658.70	<0.01	<0.01	<0.01
KC16152	658.70 ~ 659.05	0.01	<0.01	<0.01

Width (m)	Depth (m)	T-Cu (%)	AS-Cu (%)	T-Co (%)
1955.82	654.35 ~ 655.30	1.71	<0.01	0.05
1.40	655.30 ~ 656.70	0.49	<0.01	0.07

Table 2-5-1 Results of Chemical Analysis of Ore Samples (7)

MJZC-12

Sample No.	Depth (m)	T-Cu (%)	AS-Cu (%)	T-Co (%)
KC16153	652.37 ~ 652.87	<0.01	<0.01	<0.01
KC16154	652.87 ~ 653.37	<0.01	<0.01	<0.01
KC16155	653.37 ~ 653.87	<0.01	<0.01	<0.01
KC16156	653.87 ~ 654.37	<0.01	<0.01	<0.01
KC16157	654.37 ~ 654.87	0.09	<0.01	<0.01
KC16158	654.87 ~ 655.17	<0.01	<0.01	<0.01
KC16159	655.17 ~ 655.67	<0.01	<0.01	<0.01
KC16160	655.67 ~ 656.17	<0.01	<0.01	<0.01
KC16161	656.17 ~ 656.67	<0.01	<0.01	<0.01
KC16162	656.67 ~ 657.17	<0.01	<0.01	<0.01
KC16163	657.17 ~ 657.67	<0.01	<0.01	<0.01
KC16164	657.67 ~ 658.37	<0.01	<0.01	0.04
KC16165	658.37 ~ 658.87	<0.01	<0.01	0.03
KC16166	658.87 ~ 659.37	<0.01	<0.01	0.02
KC16167	659.37 ~ 659.87	<0.01	<0.01	0.01
KC16168	659.87 ~ 660.37	<0.01	<0.01	0.01
KC16169	660.37 ~ 660.87	<0.01	<0.01	0.01
KC16170	660.87 ~ 661.46	<0.01	<0.01	0.04
KC16171	661.46 ~ 661.96	1.49	<0.01	0.11
KC16172	661.96 ~ 662.46	0.01	<0.01	0.02
KC16173	662.46 ~ 662.96	0.33	<0.01	0.02
KC16174	662.96 ~ 663.46	0.29	<0.01	0.01
KC16175	663.46 ~ 663.96	0.18	<0.01	0.01
KC16176	663.96 ~ 664.37	0.29	<0.01	0.02
KC16177	664.37 ~ 664.87	0.07	<0.01	0.01
KC16178	664.87 ~ 665.37	0.12	<0.01	0.02
KC16179	665.37 ~ 665.87	0.18	<0.01	0.02
KC16180	665.87 ~ 666.37	0.12	<0.01	0.01
KC16181	666.37 ~ 666.87	0.14	<0.01	0.01
KC16182	666.87 ~ 667.37	0.13	<0.01	0.01
KC16183	667.37 ~ 667.87	0.29	<0.01	0.01
KC16184	667.87 ~ 668.37	0.03	<0.01	0.02
KC16185	668.37 ~ 668.87	0.28	<0.01	0.01
KC16186	668.87 ~ 669.14	0.34	<0.01	0.02
KC16187	669.14 ~ 669.64	1.19	<0.01	0.03
KC16188	669.64 ~ 670.14	0.54	<0.01	0.01
KC16189	670.14 ~ 670.45	0.50	<0.01	0.02
KC16190	670.45 ~ 670.95	0.65	<0.01	0.03
KC16191	670.95 ~ 671.45	0.66	<0.01	0.01
KC16192	671.45 ~ 671.95	0.85	<0.01	0.01
KC16193	671.95 ~ 672.24	0.98	<0.01	0.02
KC16194	672.24 ~ 672.74	2.86	<0.01	0.02
KC16195	672.74 ~ 673.24	1.30	<0.01	0.02
KC16196	673.24 ~ 673.74	2.68	<0.01	0.10
KC16197	673.74 ~ 674.14	0.46	<0.01	0.02
KC16198	674.14 ~ 674.64	0.01	<0.01	<0.01
KC16199	674.64 ~ 675.14	<0.01	<0.01	<0.01

Sample No.	Depth (m)	T-Cu (%)	AS-Cu (%)	T-Co (%)
KC16200	675.14 ~ 675.64	<0.01	<0.01	<0.01
KC12201	675.64 ~ 676.14	<0.01	<0.01	<0.01
KC12202	676.14 ~ 676.46	<0.01	<0.01	<0.01
KC12203	676.46 ~ 676.96	<0.01	<0.01	<0.01
KC12204	676.96 ~ 677.46	<0.01	<0.01	<0.01
KC12205	677.46 ~ 677.96	<0.01	<0.01	<0.01
KC12206	677.96 ~ 678.76	<0.01	<0.01	<0.01

Width (m)	Depth (m)	T-Cu (%)	AS-Cu (%)	T-Co (%)
3.10	669.14 ~ 672.24	0.77	<0.01	0.05
1.50	672.24 ~ 673.74	2.28	<0.01	0.05

Chapter 5 Comprehensive Analysis of the Survey Result

5-1 Geologic Structure, Characteristics of Mineralization and Mineralization Control

5-1-1 Zambian Copperbelt

The mineral deposits of the Zambian Copperbelt occur along two NW-SE trending linear zones, namely one along the western limb of the Kafue Anticline and the other along the Mufulira Syncline, as shown in Figure 1-2. The deposits occur in this belt which continues for several hundred kilometers and extend into Zaire. The mineralized zone of the Chambishi Southeast area occurs in the zone along the western flank of the Kafue Anticline. In the Zambian side, most of the copper deposits occur in the Ore Formation of the Lower Roan Group, and are clearly bounded stratigraphically. The above alignment of the deposits parallel to the Kafue Anticlinal axis is the direction of the strike of the country rock formations which is parallel to the palaeo-coastline at the time of mineralization. The continuation of the individual deposits is several to over ten kilometers in the direction of the above coastline, while that in the direction normal to the coast (toward the central part of the basin) is shorter, in the order of several hundred meters to several kilometers.

5-1-2 Ore deposit and country rock

In the Chambishi Southeast area, the orebodies occur in argillites and dolomites, and locally the mineralization also occurs in the Footwall Quartzite. It is inferred from the above that the orebodies were deposited under the shallow marine or lagoonal environment near the coast during the early stage of marine transgression. This is the stage which began with the deposition of the conglomerates of the Footwall Formation. The argillites contain large amount of organic carbon which indicates stagnant reducing environment during mineralization.

Also the sulfide minerals are distributed zonally from the coast outwards as follows; bornite → chalcopyrite → chalcopyrite-pyrrhotite-pyrite → pyrite-pyrrhotite. This indicates that the sea bottom environment, namely the environment for mineralization, gradually became reducing toward the offshore

(Fleischer et al., 1976).

5-1-3 Basement and ore deposit

The Northern Area Shoot, the most important ore deposit of the area, occurs in the depression of the basement. And the ore grade is low to barren where basement is inferred to have been high at the time of ore deposition. This inference is made from distribution of the bioherm and thickness of the Footwall Formation. This is considered to be the result of stagnant water, retention of mineralizing fluid, biogenic formation of reduced sulfur, formation of heavy metal sulfides, and thus favorable environment for the preservation of metallic sulfide in the local depressions of the basement.

It is inferred from the contour map of the upper surface of the basement that: the rise of the basement on the southwestern side of the NW-SE trending depression occur clearly. The Northern Area Shoot occurs in this depression, and it is shown that this depression is closed; the extensive palaeo-basement highs at the time of ore deposition occur in the NW-SE extending basement high on the northwest side of the Northern Area Shoot; almost NE-SW extending local depression occur in the west survey area; the basement high between Northern Area Shoot and Southern Area Shoot extends further southward, and local depression occur in the NE-SW direction between MJZC-11 and MJZC-12.

It should be noted, however, that the present morphology of the upper surface of the basement does not necessarily reflect the conditions at the time of ore deposition. There are two types of basement rise; one which coincides with the palaeo-basement highs at the time of ore deposition and the other risen by folding after the deposition of the Ore Shale. Parts of the palaeo-basement highs corresponds to the present depressions and the limbs of the depressions. In some parts of the ore horizon, dolomite overlaps with the ore-bearing argillites, and thus it is inferred that the depth of the sea changed by the vertical movement of the basement after the start of ore deposition.

5-1-4 Diagenesis, metamorphism and mineralization

The mode of occurrence of the ore shoots suggests that diagenesis and metamorphism played important roles in their formation. Although of a different type, the importance of diagenesis for the formation of Kuroko deposits which deposited on the sea floor in Neogene Tertiary has been reported (Sugawara et al., 1982). Water escape structure (Lowe et al., 1974) similar to those in the sulfides of the Kuroko ores is observed in the ores of the present area, and it is certain that the proto-ore consisting of minute sulfide grains migrated during the dehydration caused by compaction after deposition. Also the geologic units of this area have been regionally metamorphosed, and the primary rocks and minerals have all been recrystallized.

5-1-5 Gravity anomalies, ore deposit and gabbro (amphibolite)

The gravity high and low zones extracted from the gravity contour maps, and the gabbro distribution and fold axes extracted from geological map are shown in Figure 1-12.

The gravity highs near the Chambishi mine coincide well with the distribution of gabbro, and those in the western and southwestern parts of the survey area coincide with the anticlinal axes. There are small-scale gravity highs corresponding to the basement high in the central part of the survey area, but gabbro also occur in this part. The gravity high on the northern side of the Northern Area Shoot occurs in the basement depression. Ore shoot does not occur in the gravity high, and the northern boundary of the Northern Area Shoot coincides very well with the southern boundary of the gravity high to the north. From the above, it is inferred that: Parts of the gravity highs indicate the occurrence of gabbro in the shallow subsurface zones. Parts of the gravity highs indicate the basement highs either formed by folding or palaeo-basement highs which existed before ore deposition. Some kind of relationship possibly exists between the distribution of gravity highs and ore shoots.

An isopach map of subsurface gabbroic bodies (accumulative thickness when there are some bodies) prepared from drilling data and the spatial relation of the gravity highs and the ore shoots are shown in Figure 1-13. It is seen from this map that: the gravity high on the northern side of the Northern Area Shoot coincides very well with the thick part of the gabbroic body; the small-scale gravity highs lying between the

Northern Area Shoot and the Southern Area Shoot do not correspond to thick gabbro, but to the basement high; the ore shoots are developed where the gabbroic bodies are thin with the exception of the eastern part of the Southern Area Shoot. The genetic relation between gabbro and ore shoots is not necessarily clear, but the following is a possibility.

The most probable reason for the lack of association of ore shoots and thick gabbroic bodies is that the heavy load of the gabbroic bodies caused the ore material to migrate to parts with lower load. This migration is inferred to have been greater in zones where the hard compact basement rocks were shallow. The eastern part of the Southern Area Shoot-I remains below gabbro, and this is probably because the basement was deep at this point. The Southern Area Shoot-I may indicate that ore shoots can be formed where the gabbroic bodies are relatively thin by the above mechanism.

There are two theories regarding the genesis of the gabbroic bodies of this area; namely magmatic intrusion and metamorphic origin. The former genesis is widely believed, but the latter cannot be totally discarded (Mendelsohn, 1961). The basis for the metamorphic origin is that; the chemical composition of the mixture of dolomite and argillite is similar to that of gabbro, the gain-size and texture of the gabbro changes irregularly and abruptly, the gabbro gradually changes to dolomite, typical skarn minerals do not occur in the vicinity of gabbroic bodies, amphibolite formed from pelitic dolomite is similar to that formed by alteration of mafic rocks. Also if gabbroic bodies are of intruded magma origin, the following hydrothermal activities and metamorphism are considered to have took part in the migration of ore materials. However, the orebodies would have been solidified by then, and so the mechanism of migration is difficult to envisage. If the gabbroic bodies are of metamorphic origin, as the distance between the dolomitic rocks and the orebodies is in the order of 500 m, it is considered that the orebodies were still in the stage of diagenesis, and horizontal movement could have been caused by the load of the dolomitic units. The age of the rocks of this area is very old, and it is difficult to clarify the relation between diagenetic, metamorphic, and igneous activities from the recrystallized units.

5-2 Mineral Potential

Zones of high potential for shale-type copper mineralization are in the limbs of palaeo-basement highs at the time of ore deposition, particularly in the local depressions parallel to the palaeo-coast lines. Also ore shoots were not formed where thick gabbroic bodies occur and in gravity highs in this area.

It is seen from the results of the surveys carried out that the palaeo-basement highs at the time of ore deposition were distributed to the southeast, north, and northwest of the Northern Area Shoot. Of the above zones, based on the confirmation of ores in boreholes MJZC-9 and NN-75, the occurrence of ore shoots of significant scale was anticipated in the limbs of the northwestern basement high. However, zones to the northwest, north, and east of this ore shoot are considered to be in the vicinity of a palaeo-basement high at the time of the ore deposition, and also the deposits to the southeast of this ore shoot is inferred to consist of low-grade pyrrhotite-pyrite ores, it is difficult to envisage the development of large scale high-grade ore deposits in these parts of the survey area. On the other hand, the zones to the south and west of MJZC-9 are not yet explored and do not contain high gravity anomalies and are in the general direction of the extension of this ore shoot, therefore it is inferred that these zones would have high mineral potential.

The five boreholes drilled in the southern limb of the basement high to the southeast of the Northern Area Shoot are located at a relative basement high and most of the mineralization in the area belong to the pyrrhotite-pyrite-chalcopyrite zone and have low copper grade. Although of small scale, however, bornite zone was located in the lowest part of "Ore Shale" and chalcopyrite zone in the footwall quartzite. The occurrence of shoots are confined to the lowest part of the "Ore Shale" and its vicinity in this area and thus it is inferred that the period of copper precipitation was probably relatively short and thus it is possible that the ore deposits could not grow very large. If there were, however, deep local depressions of the sea floor at the time of ore deposition, it also would be possible to have formed relatively large ore shoots regardless of the length of precipitating time. From the above, the local basement depression inferred to exist to the south-southwest of MJZC-2 which confirmed relatively high-grade

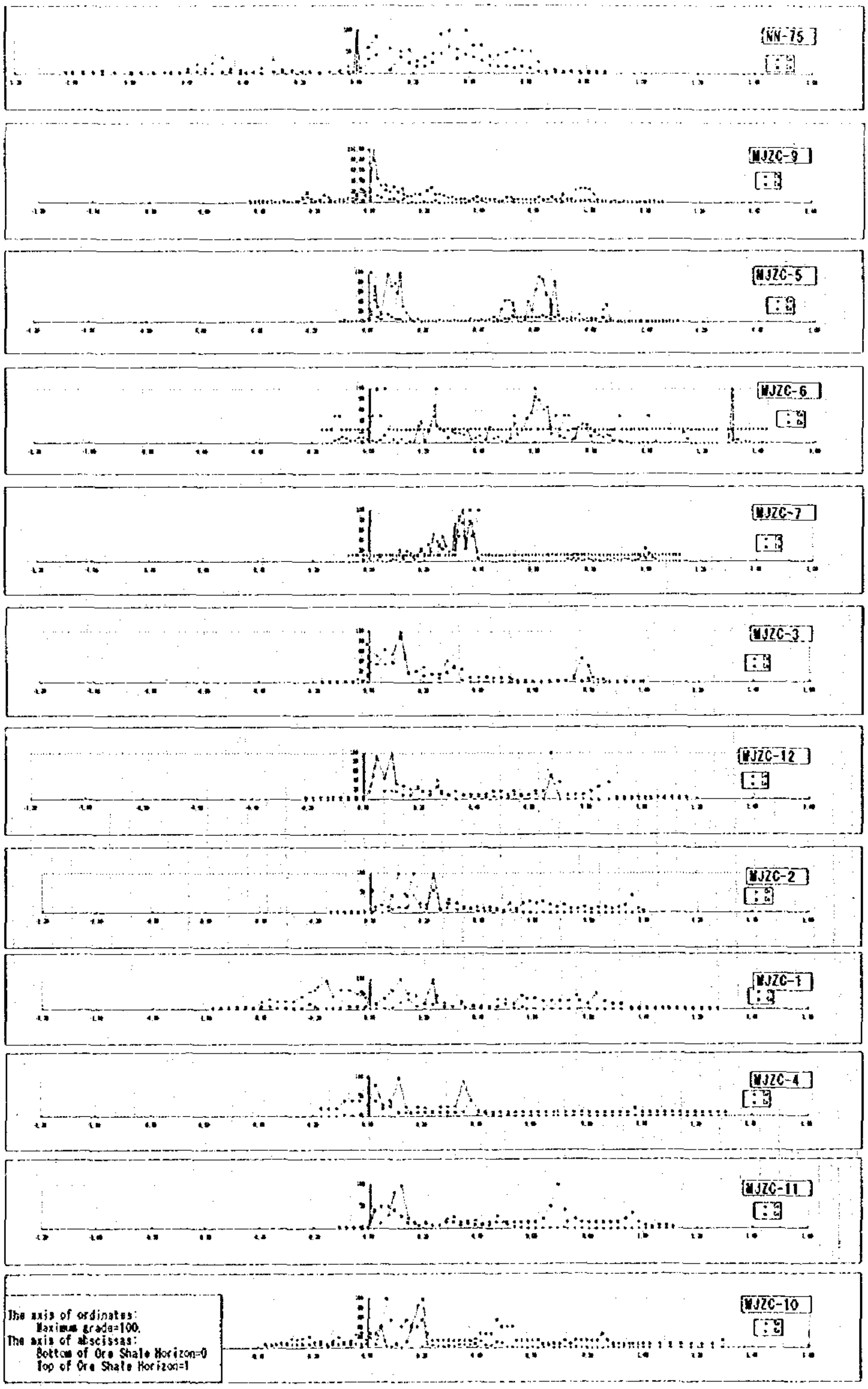

Fig. 2-5-1　Stratigraphic Correlation of Ore Grade

Table 2-5-2 Stratigraphic Correlation of Mineralization

Drill Hole No.	MJZC-1	MJZC-4	MJZC-2	MJZC-3	MJZC-5	MJZC-6	MJZC-7	MJZC-9	MJZC-10	MJZC-11	MJZC-12	NN-75	r
LOS Depth-Top (m)	504.1	919.4	638.2	632.4	967	969.5	923.8	1079.5	961.3	637.2	655.4	953.9	
LOS Depth-Bottom (m)	520.9	937.4	658.6	649.7	1005.1	1002.9	963.5	1112.2	987.4	656.6	674.1	971.35	
LOS Wd (m)	16.8	18	20.4	17.3	38.1	33.4	39.7	32.7	26.1	19.4	18.7	17.45	0.13377
LOS I-A ( )	85	85	72	85	45	58	45	60	85	83	80	70	
LOS True-Wd (m)	16.7	17.9	19.4	17.2	26.9	28.3	28.1	28.3	26.0	19.3	18.4	16.4	
Top-Cu Min(t-Cu>0.1%) *	0.557	0.403	0.562	0.795	0.864	0.896	1.033	1.000	0.489	0.559	0.675	0.755	0.42017
Bottom-Cu Min *	-0.573	-0.032	0.004	-0.008	-0.105	-0.133	0.002	-0.292	-0.389	0.005	-0.002	-0.891	-0.6761
Cu Min. Range *	1.130	0.435	0.558	0.803	0.969	1.029	1.031	1.292	0.878	0.554	0.677	1.646	0.80685
Cu m% of Cu Min *	5.124	1.462	10.658	6.751	21.051	11.950	12.172	34.517	6.421	4.562	8.029	31.651	0.98297
Co m% of Cu Min *	0.365	0.086	0.667	0.768	0.759	0.223	0.293	1.201	0.343	0.280	0.294	1.216	0.90129
Top-Co Min(t-Co>0.01%) *	0.914	0.078	0.995	0.847	0.838	0.717	0.397	1.031	0.869	1.085	0.878	0.870	0.19937
Bottom-Co Min *	-0.424	-0.196	0.004	-0.058	-0.015	-0.133	0.304	-0.445	-0.006	0.005	-0.002	-1.077	-0.7843
Co Min. Range *	1.338	0.274	0.991	0.905	0.853	0.850	0.093	1.476	0.875	1.080	0.880	1.947	0.70006
Top Depth-Cu Shoot (m)			653.83	647.73	979.55	981.40	948.45	1085.68	982.20	654.35	672.24	960.66	0.56189
LOS Upper Than Top Cu-Shoot (m) *			15.63	15.33	12.55	11.90	24.65	6.18	20.90	17.15	16.84	6.76	-0.7886
Top-Cu Shoot(t-Cu>1%) *			0.233	0.113	0.670	0.643	0.379	0.811	0.199	0.115	0.099	0.641	0.78499
Bottom-Cu Shoot *			0.079	-0.008	0.009	0.567	0.304	-0.177	0.160	0.067	0.019	-0.593	-0.746
Total Cu m%-Cu Shoot *	0.000	0.000	6.940	3.243	16.312	3.251	5.314	25.600	1.645	1.622	3.420	26.659	1
Total Co m%-Cu Shoot *	0.000	0.000	0.377	0.384	0.345	0.020	0.071	0.509	0.035	0.047	0.070	1.070	0.84154
Max Cu-Peak *	0.232	0.108	0.233	0.113	0.112	0.598	0.363	0.013	0.199	0.115	0.099	0.000	-0.5345
(Shoot/Min: Cu-m%)*100 (%) *	0	0	65	48	77	27	44	74	26	36	43	84	0.88137
(Co/Cu: Cu Min-m%)*100 (%) *	7	6	6	11	4	2	2	3	5	6	4	4	-0.2918
(Co/Cu: Cu Shoot-m%)*100 (%) *			5	12	2	1	1	2	2	3	2	4	-0.1072
ABS(Top Co-Top Cu) *	0.357	0.325	0.433	0.052	0.026	0.179	0.636	0.031	0.38	0.526	0.203	0.115	-0.5491

Abbreviation

LOS: Ore Shale Horizon I-A: Intersection angle Min: Mineralized zone ABS: Absolute value

m%: Metal content r: a correlation coefficient with Cu content of Cu ore shoot

* : Number shows stratigraphic position in the case where bottom of LOS is 0 and top of LOS is 1.

copper is noteworthy. Presence of bornite was confirmed at MJZC-12 and the occurrence of palaeo-basement high near this borehole became a possibility. The occurrence of an anticlinal axis extending in approximately north-south direction is anticipated to the south of MJZC-12, and the basement high of this area is inferred to extend further southward. Therefore, the palaeo-basement highs are distributed in relatively shallow seas to the south of MJZC-12 and the occurrence of ore shoots of the chalcopyrite zone is a possibility.

The stratigraphic positions of geologic characteristics relevant to mineralization were extracted from the cores drilled during the present survey and NN-75. The thickness of the "Ore Shale Horizon" (LOS) of each hole were used as standard with minimum LOS as 0 and Maximum LOS as 1 (Fig. 2-5-1, Table 2-5-2).

The geologic characteristics relevant to mineralization are interpreted from the above drill cores and shown in Table 2-5-2. Of these, those common to the cores with high-grade ore shoots (NN-75, MJZC-9) are as follows.

1) Copper and cobalt mineralization started early.
2) Stratigraphic range of Copper and cobalt mineralization is wide.
3) Copper and cobalt contents (m x %) of the whole copper mineralized zones are relatively high.
4) The top of the ore shoots (T-Cu>1%) is stratigraphically high.
5) The bottom of the ore shoots (T-Cu>1%) is stratigraphically low.
6) Cobalt content (m x %) of the copper ore shoots is relatively high.
7) Highest copper grade occurs near the minimum LOS.
8) The metal content (m x %) of the ore shoots occupies a relatively large part of the total metal content (m x %) of the whole copper mineralized zone.
9) The upper limits of Cu and Co mineralizations are relatively close.

We believe that when many of the above characteristics are strongly observed, the vicinity of such boreholes would be worth exploring even when the site itself is low grade. Based on the above line of thinking, the vicinity of MJZC-3 and -6 would be most promising followed by MJZC-1, -2, -7, and -12.

These drill site have considerable significance, and in particular MJZC-2, -3, -7 and -12 confirmed the local existence of high-grade ore (T-Cu>2%) and they could have penetrated the edge of ore shoots although the mineralized zones are thin.

PART III

CONCLUSIONS AND RECOMMENDATIONS

PART III Conclusions and Recommendations

CHAPTER 1 Conclusions

During the course of the three year period of Fiscal 1993 to 1995 of the Chambishi Southeast area mineral exploration, drilling, and compilation and interpretation of existing data were carried out with the following conclusions.

1. All twelve boreholes drilled during this survey attained their objectives by penetrating the ore horizon. The nine boreholes reached the basement. The geology and mineralization of the survey area were thus clarified.

2. MJZC-9 drilled in the western part of the area confirmed the existence of high-grade ores (i. width 5.90m, grade T-Cu 3.12%, T-Co 0.08%; ii. width 2.58m, grade T-Cu 2.29%, T-Co <0.01%). These ores are considered to be continuous to the shoot confirmed to the north of this hole (NN-75). Thus it is now clear that ore shoot of considerable scale exists in this area. It is inferred that this ore shoot is emplaced over a basement depression which is elongated in the NE-SW direction and it is deemed possible that this shoot is developed further southward or westward.

3. The known areal extent of the Northern Area Shoot, which is the most important ore deposit of this area, expanded northwestward by the confirmation of ores by MJZC-5 (i. width 3.10m, grade T-Cu 1.93%, T-Co 0.03%; ii. width 2.64m, grade T-Cu 2.32%, T-Co 0.03%), while it shrank in the western and southeastern parts by the confirmation of low-grade ores of MJZC-4 and barren zone of MJZC-8.

4. The five boreholes drilled in the southern part of this area (MJZC-2, -3, -11, -12) were located in relatively raised basement areas, and they showed that many of the mineralized zones consisted of low-grade copper ores belonging to the pyrrhotite-pyrite-chalcopyrite zone. But in some parts, small bornite zone in the lowermost part of the "Ore Shale" (MJZC-12), chalcopyrite zone in the footwall quartzite (MJZC-1), and local high-grade copper of pyrrhotite-pyrite-chalcopyrite zone (MJZC-2, -3, -12) were confirmed. In this area, the occurrence of ore shoots is limited only to the lowermost part of the "Ore

Shale", and thus it is inferred that ore deposition occurred in relatively short period of time, thereby limiting the size of the ore deposits. If, however, deep local depression existed on the seafloor at the time of copper deposition, relatively large ore shoots could have been formed.

5. It is inferred from distribution of the bioherm and thickness of the Footwall Formation that there was a palaeo-basement high at the ore-forming time in this area. The Northern Area Shoot which is the most important deposit of the area occurs in the depressions of the basement. And the grade of the horizon above the palaeo-basement high is low or barren. This is inferred to be the result of the formation of environment favorable for deposition and preservation of sulfides in these submarine depressions by accumulation of heavy-metal-bearing dense solutions and formation of reduced biogenic sulfur in the stagnant sea water in these local troughs.

6. In almost all of the boreholes, stratigraphic zonal arrangement of the sulfide minerals is observed in the mineralized zones. The depth of the sea probably increased after the deposition of the "Ore Shale", because the Fe/Cu ratio generally increases upward from near the lowermost part of the "Ore Shale Horizon". Most of the ore shoots in this zone belong to the chalcopyrite zone, but the high cobalt zones exist not only in the chalcopyrite, but also in the pyrrhotite and pyrite zones. It is inferred that the chalcopyrite zone was formed within a narrow sea depth zone. Therefore, we believe that the conditions for the formation of copper ore shoots would be; the continuation of the optimum depth range of the sea, and the existence of depressions suitable for the deposition and preservation of copper minerals.

7. The mode of occurrence of the rich orebodies indicate that diagenesis and metamorphism played important roles in the formation of ore shoots. Structures similar to water-escape structures of Kuroko (sulfide) deposits occur in these orebodies and the minute grain-sized sulfide proto-ore definitely migrated in conjunction with dehydration during the compaction after deposition.

8. There are two types of present basement highs, namely those which coincide with the palaeo-basement highs and those which were formed by the apparent rise of the basement by folding

after the deposition of the ores. Rich ore could occur higher than the top of the latter type highs.

9. The following is inferred from the gravity contour maps, geological maps, and drilling data. Parts of the high gravity anomalies reflect the gabbroic bodies in shallow subsurface zones. Parts of the gravity high anomalies reflect the basement highs such as the relative rise by folding and palaeobasement highs. High-grade ores most probably do not exist at gravity highs which coincide with thick gabbroic bodies. The relatively thin and low-grade orebodies deposited over the tops and limbs of the palaeo-basement highs may turn out to be rich orebodies under relatively thin gabbroic bodies.

10. Ore reserve estimation was carried out to asses the mineral potential of the survey area with the following results.

POTENTIALLY ECONOMIC MINERALIZATION;
NORTHERN AREA SHOOT: 54,793,000 tons, 2.70% T-Cu, 0.13% T-Co
SOUTHERN AREA SHOOT: 14,934,000 tons, 2.19% T-Cu, 0.13% T-Co
SUBECONOMIC MINERALIZATION :
107,909,000 tons, 1.83% T-Cu, 0.03% T-Co

CHAPTER 2 Recommendations for Future Exploration

Significant amounts of ore were confirmed in this survey area by drilling during this year. The ore deposits of this area, however, occur in relatively deep zones, the major deposits probably occurs at 550 to 1,050m below the surface. Therefore, in order to develop this deposit, it is necessary to further increase the ore reserves. The western and southern parts of the survey area have not been explored and the potential is considered to be promising.

It is now clear, from the results of the present survey, that a deposit which was hitherto unknown occurs in the western part of the area. Also borehole RCB-2 which previously confirmed ores is located far south of MJZC-9 which also confirmed ores. From the above it is strongly recommended that efforts be concentrated as follows to confirming new ore reserves and to exploring the vicinity.

First drill at sites where the depth of the ore deposits can be estimated at shallow depths, namely near the two boreholes which encountered ores (MJZC-9, NN-75), then drill at sites where the depth of the ore is considered to become deeper, namely south and west of MJZC-9.

The possibility of ore shoots still remain in the southern part of the area and thus it is recommended that drilling be carried out in the area to the south of MJZC-12.

Also in order to accurately determine the ore reserves of the Northern Area Shoot, the main deposit, drilling should be carried out near the peripheries of the deposit.

REFERENCES

R E F E R E N C E S

Fleischer, V.D., Garlick, W.G. and Haldane, R. 1976. Geology of the Zambian Copperbelt, Handbook of Strata-bound and Stratiform Ore Deposits (K. H. Wolf, ed.), Elsevier, Amsterdam, vol.6, p.223-350

Fleischer, V.D. 1983. Discovery of a New Copper-Cobalt Sulphide Occurrence in the Chambishi Basin, Zambia, Central Africa. Paper presented at "Proterozoic '83", Lusaka, Zambia

Garlick, W.G. 1964. Association of Mineralization and Algal Reef Structures on Northern Rhodesian Copperbelt, Katanga, and Australia. Econ. Geol., vol.59, p.416-427.

Lowe, D. R. 1975. Water escape structures in coarse-grained sediments. Sedimentology, vol.22, p.157-204.

Malan, S.P. 1964. Stromatolites and Other Algal Structures at Mufulira, Northern Rhodesia. Econ. Geol., vol.59, p.397-415.

Mendelsohn, F. 1961. The Geology of the Northern Rhodesian Copperbelt, ed. F. Mendelsohn. Macdonald and Co. London. 523 pages.

Sugawara, M., Sato, K., Sato, S. and Nagasaki, N. 1982a. Mode of Occurrence of the Shakanai Kuroko Deposits with Special Reference to Some Sedimentological and Diagenetic Features - Studies on Diagenesis of Kuroko Deposits (Description). Mining Geology, vol.32, p.305-322 (in Japanese).

.... 1982b. An Attempt to Reconstruct the Diagenetic Evolution History of the Shakanai Kuroko Deposits - Studies on Diagenesis of Kuroko Deposits (Discussion). Mining Geology, vol.32, p.405-415 (in Japanese).

Zambia Consolidated Copper Mines Limited 1993. Proposal for a Mineral Exploration Project to be Carried out by the Metal Mining Agency of Japan and the Japan International Co-operation Agency on the Chambishi Southeast Deposit, Copperbelt Province, Republic of Zambia.